

ABSTRACT

LEE, JOO HONG. A Study of Solid State and Solution State of Residual Hemicellulose from Dissolving Pulp. (Under the direction of Dr. Sunkyu Park and Dr. Stephen Kelley).

A dissolving pulp is a premium quality of pulp that typically has more than 95% cellulose and less than 5% hemicellulose. There are many value-added applications for this high-quality dissolving pulp including production of cellulose esters, e.g., cellulose acetate, propionate, and butyrate. However, even with the long history of the cellulose ester industry, there are unresolved issues on how the quality of the dissolving pulps impacts the quality of the ester product. Specifically, after the commercial acetylation process there can be acetone insoluble particles, “gels”, that can cause problems in subsequent processes such as fiber spinning or casting transparent films. Many studies have attributed these gels to the residual hemicelluloses in the dissolving pulps. Therefore, the goal for this project is to understand the relationship between the chemical structure of the residual hemicelluloses, and the properties of acetylated hemicelluloses in solid and solution state.

Four hemicelluloses were studied, one isolated from a commercial process, and three extracted from commercial dissolving pulps using a high concentration of potassium hydroxide. All were dissolved in an ionic liquid and then acetylated to a controlled degree of substitution (DS). After acetylation, $^1\text{H-NMR}$ was used to characterize the acetylated product. However, there were limitations to using NMR, because some of the hemicellulose acetates were not soluble in NMR solvents. Therefore, a new analytical method was developed to characterize the acetyl DS in the solid state. FTIR with multivariate analysis was used to relate changes in the IR spectral to the hemicellulose DS.

In addition, X-ray diffraction (XRD) was used to study the relationship between the starting hemicellulose, its DS and the degree of ordering for several hemicellulose acetates. The crystallinity of hemicellulose and hemicellulose acetate have not been studied widely, especially hemicellulose isolated from dissolving pulp. The XRD showed that partial acetylation reduced order, but at high DS levels some hemicelluloses could form new crystalline structures.

Finally, the solution properties of the cellulose and hemicellulose acetates were examined with dynamic light scattering to evaluate the role of residual hemicellulose. It was difficult to obtain homogeneous solutions of the hemicellulose acetates. Commercial cellulose acetates with different amounts of “gel” or hemicellulose acetates were studied, and the DLS measurements

suggest that the hemicellulose acetates are not easily dissolved in acetone, and can interfere with the behavior of the cellulose acetates.

A thorough analysis of hemicelluloses with differing DS levels using FTIR, NMR, XRD, and DLS, showed that the solubility and crystallinity of hemicellulose acetates were heavily influenced by the DS, and the composition of the original hemicellulose.

© Copyright 2019 by Joo Lee
All Rights Reserved

A Study of Solid State and Solution State of Residual Hemicellulose from Dissolving Pulps.

by
Joo Hong Lee

A thesis submitted to the Graduate Faculty of
North Carolina State University
in partial fulfillment of the
requirements for the degree of
Master of Science

Forest Biomaterials

Raleigh, North Carolina
2019

APPROVED BY:

Sunkyu Park
Committee Co-Chair

Stephen Kelley
Committee Co-Chair

Hassan Jameel

DEDICATION

I would like to dedicate this accomplishment to my family. They always provided me with unconditional love and care under any circumstances. To Mia Kwon, for your unstoppable attention and care for me. To my close friends, Daniel, Jake.1, Jake.2, Jessie, Danny, and Raymond, for your continuous support and love for me. Finally to God, who's been giving me all the strength I need to accomplish this achievement.

BIOGRAPHY

Joo was born in Daegu, South Korea on September 6, 1992. He grew up in Korea until the age of 13 and immigrated to Prince George County, VA, United States. Joo finished his middle school, junior high school, and high school in Prince George. Throughout his high school career, his favorite activity was playing tennis and participating in local tennis tournaments.

After high school, Joo received and accepted an admission to North Carolina State University studying B.S. Paper Science Engineering and B.S. Chemical Engineering. Throughout the college, he worked at Loparex as an internship, co-op at WestRock, and worked as a research assistant at university in Dr. Park's laboratory. After receiving his diploma in both Paper Science Engineering and Chemical Engineering degree, he made a decision to study further about different applications of forestry by applying the graduate school at Forest Biomaterials at North Carolina State University.

Currently, he is studying at NC State pursuing his Master of Science degree, and upon his graduation at NC State, he has received and accepted an offer to work as Chemical Engineer at Eastman Chemical Company in Fall 2019.

ACKNOWLEDGMENTS

I would like to acknowledge Eastman Chemical Company for their research grant to support me all throughout the past two years in order to achieve this M.S. degree. Special thanks to Trevor Treasure, Jennifer Skotty, Barclay Satterfield, and Kate Kornau, for being on the conference call every other Friday for the past two years.

I foremost would like to thank Dr. Sunkyu Park and Dr. Kelley for your time and presence during and outside of discussion with Eastman. Without both advisors, this chapter of my life would have really been impossible. I have been very fortunate to have them as my advisors and mentors here at NC State.

Finally, I want to give thanks to Dr. Chaehoon Kim. He supervised me when I first came into the laboratory. He taught me how to interpret and think critically and taught me all the detail things about laboratory and planning experiments. Without his guidance from the beginning, these two years of the journey would have been truly impossible.

TABLE OF CONTENTS

LIST OF TABLES	vii
LIST OF FIGURES	viii
Chapter 1: Review of the articles.....	1
Process of making cellulose acetate.....	1
Gel particle from cellulose acetate.....	3
Residual hemicellulose from dissolving pulp and their characteristic.....	5
Chapter 2: Development of a new quantitative method for measuring the DS of acetylated xylan7	
Introduction.....	7
Experimental methods and materials	9
Materials	9
Extraction of hemicellulose from dissolving pulps	10
Compositional analysis using ion chromatography	11
Synthesis of ionic liquid.....	11
Dissolution and acetylation of hemicellulose	11
Fourier Transform Infrared spectroscopy	12
Proton Nuclear Magnetic Resonance (¹ H-NMR)	12
Principal Component Analysis (PCA) & Partial Least Square (PLS) statistical analysis	12
Result and discussion.....	13
Proton Nuclear Magnetic Resonance (NMR).....	15
Discussion of characteristic peaks from FTIR-ATR	16
Principal Component Analysis	18
Discussion of partial least squares regression analysis.....	21
PLS factor 1 models.....	22
PLS factor 2 model for HW+SW+CA	24
Prediction results of developed PLS models	25
Conclusion	28
Chapter 3: Crystallography study of hemicellulose and related solubility.....	30
Introduction.....	30
Experiment methods and materials.....	31
Extraction of hemicellulose from dissolving pulps	32
Composition analysis of extracted hemicelluloses	32
Synthesis of ionic liquid.....	33
Dissolution and acetylation of hemicellulose	33

Fourier Transform Infrared spectroscopy (FTIR).....	33
Proton Nuclear Magnetic Resonance (¹ H-NMR)	34
X-ray Diffraction Analysis	34
Glycosidic linkage analysis.....	34
Solubility visual inspection.....	35
Result and discussion.....	35
Characterization of acetylation reaction by FTIR and ¹ H-NMR	36
Discussion of insolubility of hemicellulose	39
X-ray diffraction of hemicellulose and acetylated hemicellulose.....	39
Discussion of solubility and crystallinity of hemicellulose	41
Conclusion	43
Chapter 4: Dynamic light scattering study of cellulose acetate in acetone solution.....	44
Introduction.....	44
Theory of dynamic light scattering (DLS).....	44
Experiment methods and materials.....	47
Materials	47
Dynamic light scattering (DLS).....	47
Insoluble gel extraction.....	48
Result and discussion.....	49
Baseline evaluation of the dynamic light scattering	49
DLS of CA-HQ and CA-LQ.....	51
DLS comparison for gel particles and gel removed.....	53
Protocol for estimating the amount of gel particle present	55
Conclusion	57
REFERECE.....	58

LIST OF TABLES

Table 1. List of dissolving pulps used and general characteristics.	10
Table 2. Composition analysis of the hemicelluloses (ND: non-detected).....	11
Table 3. Experimental condition for all samples... ..	13
Table 4. List of characteristic peaks for glucan/xylan and acetylated glucan/xylan.	17
Table 5. List of glucan and xylan backbone region FTIR vibrations for different compounds. ..	21
Table 6. List of R-squared and RMSE value for all three models.....	25
Table 7. Composition analysis result for the hemicelluloses.....	33
Table 8. Experimental condition for hemicelluloses.	36
Table 9. List of samples and descriptions for DLS experiment.....	49
Table 10. Amount of acetone added to dilute 1.0% to 0.1 - 0.9% solutions.	52
Table 11. Gel ratio and hydrodynamic size for each sample.....	53

LIST OF FIGURES

Figure 1. $^1\text{H-NMR}$ spectra of HW2-MR0.75, MR1.3, and MR1.6, from bottom to top.....	15
Figure 2. Area normalized ATR-IR of HW2 and acetylated HW2.	18
Figure 3. PCA score plots from the FTIR spectra of native and acetylated hemicelluloses.....	19
Figure 4. PCA-PC1 loading plots for the samples shown in Figure 3.	19
Figure 5. PCA-PC2 loading plots for the samples shown in Figure 3.	20
Figure 6. The regression coefficients for all developed models.	22
Figure 7. PLS regression result for HW+SW factor 1 (HS-1) model.	23
Figure 8. PLS regression result for HW+SW+CA factor 1 (HSC-1) model.	24
Figure 9. PLS regression result for HW+SW+CA factor 2 (HSC-2) model.	25
Figure 10. Prediction result using HS-1 model.	26
Figure 11. Prediction result using HSC-1 model.	27
Figure 12. Prediction result using HSC-2 model.	28
Figure 13. FTIR spectra for HW at different DS.	37
Figure 14. H-NMR spectra of a) HW and b) HW-MR1.3 in DMSO- d_6	38
Figure 15. H-NMR spectra of SW in DMSO- d_6	38
Figure 16. X-ray diffraction graph for the native and acetylated HW samples.	41
Figure 17. X-ray diffraction for the native and acetylated SW samples.	41
Figure 18. Time depended fluctuation of small and large particles.	45
Figure 19. An example of a correlogram result.	46
Figure 20. Schematic of cellulose acetate solution gel extraction and experimental method.	48
Figure 21. Size distribution by intensity graph for polystyrene materials.	50
Figure 22. A mixture of PS-13K and PS-290K.	50
Figure 23. DLS measurement for CA-HQ and LQ before gel removal.	51
Figure 24. CA-LQ with different amount of gels.	54
Figure 25. CA-HQ with different amount of gels.	55
Figure 26. Calibration curves for CA-LQ (red) and CA-HQ (blue).	56

Chapter 1: Review of the articles

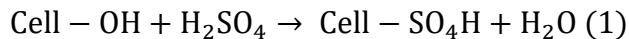
Process of making cellulose acetate

Cellulose esters serve a variety of applications in food, cosmetic, clothing, pharmaceutical, coatings, films, etc. Within product lines of cellulose esters, there are different kinds of cellulose esters and mixed esters. Cellulose acetate homopolymers and , cellulose acetate propionate, and cellulose acetate butyrate copolymers are the common commercial cellulose esters. The chemical reaction between cellulose and various anhydrides ester has been around more than a century and there have been numerous fundamental, application, and review works done on in the past. There continue to be innovative and detailed new research coming every year. Therefore, it is important to understand the molecular level details behind this basic methodology of cellulose acetate.

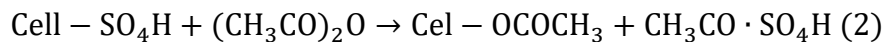
United States Patent (Patent Number: 5608050)¹, provides a general description of the cellulose acetylation process. First, the cellulose raw materials must be activated by mixing with water, aqueous acetic acid, or a small amount of sulfuric acid. To initiate the acetylation reaction, cellulose is mixed with a mixture of prechilled acetic anhydride, acetic acid, and sulfuric acid to produce cellulose triacetate. Produced triacetate may be subjected to hydrolysis to produce cellulose acetate of lower acetyl content¹. When producing commercial grade cellulose acetate, it is important to use dissolving pulp, which has high alpha cellulose content and usually hemicellulose content of 5 % or lower. Using high purity pulp can eliminate potential by-products that could harm the process down the line. The acetylation step in a typical industrial cellulose acetate process is highly exothermic therefore, all using chemicals and the reactors need to be cooled to prevent overheating, and subsequent cellulose backbone hydrolysis and other side reactions¹. The typical industry process requires the use of a sulfuric acid catalyst (6 to 20%) to uniformly acetylated the cellulose and synthesized cellulose acetate can have good solubility in an acetic acid system. The sulfuric acid is neutralized and then must be washed thoroughly to prevent the poorly sulfate salts from plugging process operations. Or, residual sulfate esters can become unstable when exposed to heat¹.

The groundbreaking work of Malm, et al,² also highlighted the details of producing cellulose acetate. In this work, the acetylation took place in water-jacketed stainless steel mixer that carefully controlled for temperature and mixing of chemicals. In process uses one part of cellulose was initially activated with 2.4 parts of acetic acid and stirred at 100 °F for ?? minutes. Then, four parts of acetic and 0.88 wt.% sulfuric acid (based on cellulose) were added and mixed at the same temperature for 45 minutes to complete the activation stage. Then the mixture was cooled to 65 °F, and 2.7 parts of 98% acetic anhydride and remaining 6.12 wt.% sulfuric acid were then added. The temperature was controlled to limit the exothermic reaction and associated temperature increase, and the final reaction temperature was held at 90 – 95 °F for 1.5 to 2 hours. At this stage, the produced cellulose acetate is cellulose triacetate dissolved in acetic acid, acetic anhydride solution. Therefore, the resulting reaction dope was viscous and free of fibers. To produce a commercially useful cellulose diacetate one part of water and two parts of acetic acid are added to back hydrolyze the cellulose triacetate to cellulose diacetate (DS=2.5).

The role of the sulfuric acid as a sulfate ester and also as a catalysis is very important and has been studied by Araki³. They show that in the reaction mixture, one mole of cellulose hydroxyl with one mole of sulfuric acid proceeded to cellulose sulfation shown by reaction equation 1.



Then, the sulfated cellulose reacted with one mole of acetic anhydride thus synthesizing one mole of acetylated cellulose and one mole of sulfated acetyl group shown by reaction equation 2.



It was reported by Araki that reaction 1 readily took place even at low temperature but the reaction 2 occurred slowly at low temperature.

Another possible route of acetylation reaction for cellulose was also proposed by Arakai³. One mole of cellulose hydroxyl reacting with one mole of acetic anhydride forming one mole of acetylated cellulose and one mole of acetic acid under an acidic condition provided by sulfuric acid. The reaction equation 3 shows the previously described reaction.



The acetylation reaction through reactions 1 and 2 and through reaction 3 took place competitively depending on reaction conditions such as temperature, the amount of acetic acid, acetic anhydride, and sulfuric acid present in the reaction mixture.

An alternative to the commercial heterogeneous reactions is the work of McCormick et al, who extensively studied homogeneous system derivatization of cellulose in lithium chloride and *N-N*-dimethylacetamide solution (LiCl/DMAc)⁴. A few advantages of performing the reaction in homogeneous phase are moderate reaction temperature, less reagent requires, less degradation of cellulose, and direct control over the DS⁴. The LiCl/DMAc solvent was prepared by mixing lithium chloride solution of concentrations 9% (w/w) and DMAc at 100 °C. The LiCl/DMAc is cooled to room temperature before it is used to dissolve cellulose, and then 0.11 mol sulfuric acid in 25 mL DMAc were added dropwise. A solution of 0.11 mol acetic anhydride was added dropwise over 1 hr, followed by constant stirring 8 h at 25 °C. The product was isolated by precipitation in hot distilled water and purified by Soxhlet extraction with methanol for 24 h, followed by drying at 60 °C for 48 h in a vacuum oven.

Gel particle from cellulose acetate

Since the 1950s many articles have reported on the behavior of insoluble “gel” particles found in the commercial cellulose acetate process. The nature of these gel particle is complex, however, there are several dominant theories.

The most common commercial process for products of acetone soluble cellulose diacetate is the controlled hydrolysis of cellulose triacetate to a DS of about 2.5. This cellulose diacetate is commonly used for the production of fibers that are spun from acetone solution using a ‘dry process’ where the acetone is evaporated from the fiber⁵. During this process, acetone insoluble particles can clog the orifice and cause disruption of the fiber formation process. Due to their commercial importance, these acetone insoluble “gel” particles have been extensively studied.

One common method to isolate these gel particles is by dissolving cellulose acetate at 3 wt.%, or higher concentration, and centrifuge the solutions at a high level of gravitational force for four hours or more. The recovered sediment at the bottom of the centrifuge tube is designated

as the 'gel' fraction. Depending on a pulp source, the composition of gel can vary, but one common observation from numerous studies is that all gel particles have a significant composition of hemicellulose, either xylose or mannose, depending on the wood species. Chen, et al., 2013, studied acetone insoluble gel particles isolated from four different cellulose fibers (cotton linter, hardwood dissolving pulp, softwood dissolving pulp, and paper grade fibers). Analysis of the monomeric sugar residues in the initial pulp materials showed the less than 3% of sugars were non-glucose sugars for the dissolving pulp grade hardwood and softwood and cotton linter, but only 81% of monomeric sugars in paper pulp were glucose⁵. This is expected since paper grade pulps maximize yield and thus do not attempt to remove many of the hemicelluloses. Relative to the starting pulp fibers, the isolated gels showed 14, 19, 26, and 68 wt.% non-glucose sugar content for the cotton, hardwood, softwood, and paper sources, respectively.

Similar composition analysis was conducted obtained for Fleury 1994⁶. His study showed that the insoluble gels isolated from cellulose diacetate contained 30% xylose and 10% mannose.

Initial work with these gels done by Bradway 1953⁷ led to a few important conclusions. The insoluble gel fractions from cellulose acetate all were in acetyl range of acetone soluble. Despite this, they were insoluble in acetone and other solvents. Re-acetylation of the gel led to better dispersibility in acetone but still, no sign of the dissolution was observed. The mannan and xylan in hazy fraction were isolated and removed which resulted in a much less turbid acetate solution. Therefore, Bradway claimed the appearance of turbidity issue in cellulose acetate in acetone solution was due to the presence of mannan and xylan fractions.

Wilson⁸ studied isolated gels and reported similar results to Bradway⁷. In addition to the study of gels he also studied the effect of pulping process on structures of hemicelluloses. Figure 2 from his report shows that hemicellulose isolated from wood pulps subjected to different pulping processes can have different hemicellulose structures. For example, softwood subjected to acid sulfate pulping will have fewer 4-O-methylglucuronoxylan, than after conventional kraft pulp, but will retain some arabinose branch groups. In the case of prehydrolysis kraft pulping arabinose groups are cleaved off resulting in a relatively linear xylan hemicellulose fraction. Glucomannan hemicellulose has branching group of galactose and acetyl group therefore, after acid sulfite or kraft or prehydrolysis kraft all resulted in less branched structure of glucomannan.

Wilson⁸ also studied the effect of residual hemicellulose on cellulose diacetate (CDA) and their impact if more hemicellulose was present within the CDA by external addition of the extracted xylan-rich or glucomannan-rich hemicelluloses. Two important highlights are the following. The external addition of 2.5 wt% of glucomannan drastically increased the false viscosity up to 400%, false viscosity refers to a drastic increase in viscosity when the concentration of a solution is raised⁶, the second, a haze density from CDA was highest when linear xylan hemicellulose was added.

In addition to reporting the monomeric sugar composition of gels, Chen, et.al.⁵, also used XRD to add extra insight into the formation of gel particles. The result of the sugar composition of insoluble gel showed 81% glucose, 19% xylose, and a trace amount of mannose. So far, previous works have proved the presence of hemicelluloses such as xylan and mannan is the main cause of gel formation. Chen analyzed the gel particles with XRD and figure 2 of his report shows the presence of cellulose microcrystalline structure. He claimed that during the heterogeneous phase acetylation process there are some inner parts of cellulose that acetylation reaction did not take place thus leaving this microcrystalline structure. Therefore, this microcrystalline structure or unreacted cellulose is also insoluble in acetone which explains the glucose portion of the sugar composition analysis.

Residual hemicellulose from dissolving pulp and their characteristic

Prior works have shown that gels are rich in hemicellulose sugars, but the detailed structure of the hemicellulose can vary widely due to the effects of different wood sources and pulping conditions, so more fundamental research is needed to better understand the gels. Gardner and Chang, and Kim et. al., used linkage analysis of residual hemicellulose isolated from dissolving pulp and attempted to identify how the detailed structure of hemicellulose can affect the gel formation⁹⁻¹⁰.

Linkage analysis is conducted using a sequence of reductions, hydrolysis, labeling reactions to transform hemicelluloses partially methylated, acetylated alditol monomer units. Then GC-MS and GC-FID can be used to identify and quantitatively assign the original

monomeric sugars and their structures. Gardner and Chang, and Kim et. al., showed that kraft pulping cleaves 4-O-methylglucuronic acid branching group from xylan, while acid sulfite pulping does not. The work of Kim, et. al., supported the conclusion that hemicelluloses isolated from kraft pulps are dominated by 1 – 4 xylan structures. Based on the GC-MS work, the acid sulfite treated hemicellulose retained a significant amount of glucuronic acids.

Gardner and Chang (1974) also examined the ordering in the hemicelluloses isolated from both kraft and acid sulfite pulps, and observed the presence of crystalline structures in kraft treated hemicellulose. Single amorphous halo was observed for acid sulfite treated hemicellulose. Similarly Horio¹¹ studied ordering in xylan isolated from wood. His findings supported the observations by Gardner and Chang. Horio found that reducing the amount of glucuronic acid branch group changed the XRD patterns from poorly organized amorphous patterns to well-defined crystalline structures

In combination these isolation and analytical methods highlight the complex relationship between the original wood sources, the commercial pulping and bleaching conditions, the method used to isolate the residual hemicellulose and the impact of the hemicellulose on the subsequent performance of derivatives made from the dissolving pulps.

Chapter 2: Development of a new quantitative method for measuring the degree of substitution of acetylated xylan

Introduction

The global demand for dissolving pulp has increased from 5.6 million tons to 7.5 million tons since 2013 due to wide range growing uses, including viscose fibers and regenerated cellulose fibers, and value-added cellulose derivatives. There has been a significant increase on demand from the countries in Asia, which is driving global demand¹². In addition to viscose, cellulose derivatives, such as cellulose esters, ethers, nitrates, etc., have continued to find new applications in materials, foods and pharmaceutical applications¹³. The increasing demand for dissolving pulp has allowed a number of mills to convert from conventional pulp processing into dissolving pulp mill¹³. However, this conversion is not easy due to high purity requirements for dissolving pulp, high α -cellulose (> 95%) and less than 5% residual hemicellulose contents. At the same time not all applications for dissolving pulp require the highest purity, and this has created interest in understanding the relationship between the process used for manufacturing dissolving pulps, and the details of the hemicellulose residues.

Unlike the pulps that used to make paper, dissolving pulps typically require very low content of hemicellulose due to the detrimental impacts of the residual hemicelluloses in many application processes. There have been several studies^{5-6, 8-9} that have highlighted the negative impact the hemicellulose in the production of cellulose esters¹⁴⁻¹⁶. Prior works have highlighted the impact of 'gel' particles on the solution properties for both cellulose esters and the Tencel process. Thus, from a commercial and theoretical perspective it is important to understand the relationship between the amount and structure of residual hemicellulose, and the performance of dissolving pulps in different applications. In the case of cellulose esters, the majority of the applications require a process stage with a homogeneous solution, e.g., for spinning fibers from acetone, or casting films from an organic solvent. In these applications an accumulation of gel particles can plug the commercial filtration process¹⁷.

A common method to study the impact of residual hemicellulose is the analysis of particles isolated from solutions. This is a ‘functional test’ since the solution properties of residual materials is a complex interaction between the solvent, process conditions, e.g., temperature, shear and concentration, the type of derivative, and the specification for the final product. Nevertheless, these gel particles are conveniently isolated by extended centrifugation^{5,7}. These studies are consistent in their conclusions that the recovered particles are rich in hemicellulose sugars, specifically xylan. Many have also concluded that a high xylan content also produces residual yellow color. Residual glucomannans have also been identified as responsible for spurious measurements of the cellulose esters solution viscosity⁸.

There is a complex interaction between the different pulping processes, e.g., prehydrolysis, kraft, or acid sulfite, wood species and targeted pulp quality attributes. For example, linkage analysis of kraft pulped xylans shows that they are rich in unsubstituted (linear) xylan units, while acid sulfite pulps have more 4-O-methyl glucuronic acid ‘side chain’ groups that are present in the ‘native’ xylans⁸⁻⁹. Previous studies have shown that the solubility of xylan acetates vary significantly depending on their solubility and MWs. The solubility of xylan acetates vary widely, with polar, aprotic solvents such as DMSO or pyridine at 80 °C being effective, and chloroform or dichloromethane being less effective. As expected the MW of xylan or xylan acetates has an important role in their solubility¹⁷. Whistler reports that high quality xylan diacetate is insoluble in most solvents, but as the MW of xylan acetate decreases, the solubility will first observe with pyridine. Further degradation of xylan acetates will then allow the xylan acetates to dissolve in chloroform.

In the production of cellulose derivatives such as cellulose acetate, it is also important to understand how behavior of the acetylated cellulose and the acetylated hemicellulose may differ. Specifically, the solubility of acetylated hemicellulose appears to be lower than that of the dominate cellulose acetate, and the lack of hemicellulose solubility as a commercial and analytical challenge. Convenient methods to quantitatively measure the degree of substitution (DS) of cellulose esters with ¹H-NMR are not directly applicable to xylan acetates since their partial insolubility makes solution NMR unreliable. Thus, there is a need for additional analytical approaches that allow precise measurement of DS insoluble samples. This work demonstrates the potential for using FTIR, combined with multivariate analysis, to predict the DS of insoluble

hemicellulose acetates, and suggests that this approach may also be widely applicable for carbohydrate esters.

Experimental methods and materials

Materials

Both hardwoods and softwoods, and a series of different, commercial pulping processes were used for this study the wood sources and pulping processes are listed on Table 1. As noted above, conventional kraft pulping is insufficient to completely remove the residual hemicelluloses. Therefore, additional pulping steps are required to produce a dissolving grade.

For example, prehydrolysis kraft, cold caustic extraction, and acid sulfite are the three main types of pulping. Depending on the desired final quality of the dissolving pulp, single or multiple pulping stages can be done. There are advantages and disadvantages associated with each types of pulping. In general, sodium hydroxide is efficient at removing both hemicellulose and lignin, but at high temperature, it can initiate the peeling reaction that will harm the total yield of the product, and at low temperature there is risks of forming high content of cellulose II and lacks an ability to extract glucomannan type hemicellulose¹⁸. Acid sulfite, on the other hand, is effective at removing both types of hemicelluloses and no formation of cellulose II, but it comes with a cost of random hydrolysis as a result of using acid, this will hurt the yield and broaden the MW distribution of the product¹⁹. Below list is the brief and common conditions for each types of pulping.

- Prehydrolysis Kraft (PHK) pulping includes either direct steaming at temperatures between 160 and 180 °C for between 30 min and 3 hours, or application of dilute mineral acid (0.3-0.5% H₂SO₄) at temperatures between 120 and 140 °C²⁰. This treatment can liberate organic acids, which can preferentially hydrolyze the more accessible hemicellulose.
- Cold caustic extraction (CCE) involves mixing the pulp with 5-10% NaOH for at least 10 minute at temperatures between 25 and 45 °C²⁰.

- Acid sulfite (AS) is a fundamentally different process that uses strongly acidic condition with a pH between 1.5 and 2, and the pulping temperature ranges from 125-145 °C for cooking time up to 7 hours²¹.

Table 1. List of dissolving pulps used and general characteristics.

<i>Sample</i>	<i>Pulping process</i>	<i>Abbreviation</i>	<i>Extraction</i>
HW1	Prehydrolysis Kraft	PHK	24% KOH
HW2	Cold Caustic Extraction/ Prehydrolysis Kraft	CCE/PHK	CCE pulping residues
HW3	Cold Caustic Extraction/ Prehydrolysis Kraft	CCE/PHK	24% KOH
SW1	Acid Sulfite	AS	24% KOH

All the pulp samples were generously provided by Eastman Chemical Co. All chemicals used for this work were purchased from Fisher Scientific or Sigma Aldrich and used without further purifications.

Extraction of hemicellulose from dissolving pulps

Hemicelluloses from dissolving pulps HW1, HW3 and SW1 were extracted using the 24% KOH extraction protocol developed by Gardner and Chang⁹. Briefly, the extraction procedure is as follows. One OD g of dissolving pulp is mixed with 20 mL of 24 wt% KOH solution containing 0.5 wt% of sodium borohydride, and left on an automatic shaker for six hours at room temperature. The dissolved hemicellulose filtrate was centrifuged and separated with a 0.2 µm nylon membrane installed the conical tube. The resulting filtrate was mixed with ethanol and acetic acid solution (9 parts ethanol and 1 part acetic acid) at a volume ratio of 5 to 1 ethanol-acetic acid solution to the filtrate. The hemicellulose was allowed to precipitate overnight. The ethanol and acetic acid solution was decanted, and precipitant was washed with ethanol three times and air dried. Only the 1st stage extraction was used for this work because xylan enriched hemicellulose portion was the focus of this study, and a ‘total’ xylan extraction was not of interest.^{10, 22}

Compositional analysis using ion chromatography

The NREL standard method²³ was used to measure the sugar content of the hemicellulose samples (Table 2). A compositional analysis following the NREL protocol was performed for all starting pulp samples to understand their total sugar composition. The monomeric sugars were analyzed using an ion chromatograph (Dionex ICS 5000, Dionex, Sunnyvale, CA, USA) equipped with an electrochemical detector (ED) and anion exchange column (Dionex CarboPac PA200)(3 x 250 mm) at 30 °C. A mobile phase used was 100 mM sodium hydroxide and standard glucose, xylose, and mannose solutions were used to create the calibration curve.

Table 2. Composition analysis of the hemicelluloses (ND: non-detected).

<i>Sample</i>		<i>Composition analysis</i>		
		Glucose (%)	Xylose (%)	Mannose (%)
HW-1	PHK	3.4	92	0
HW-2	CCE/PHK	2.1	94.8	0
HW-3	CCE/PHK	14.6	76	1.9
SW-1	AS	15.4	53.6	11.4

Synthesis of ionic liquid

The acetylation of all hemicellulose samples was carried out in [DBNH][OAc] ionic liquid (IL). Synthesis of the IL is as follows: mix equimolar of DBN and acetic acid in an ice water bath, and flush the IL containing glass vial with nitrogen gas and sealed²⁴. The cooling and nitrogen atmosphere were needed to limit the exothermic reactions from the synthesis of the IL, and minimize the formation of side-products²⁴.

Dissolution and acetylation of hemicellulose

Complete dissolution of hemicellulose in the IL varied depending on sample types. Typically, two hours of dissolution time was enough to obtain complete dissolution. Solutions with 5 wt% hemicellulose in IL were prepared, e.g., 80 mg of hemicellulose was dissolved into 1.6 g of the IL at 80°C for two hours.

Then, following the protocol developed by Stepan 2013²² acetic anhydride (Ac₂O) was added to initiate the acetylation reaction. The DS was controlled by varying the mole ratio of hemicellulose hydroxyl groups and Ac₂O. For example, HW2 has 1.22 mmol of hydroxyl groups per 80 mg. The target mole ratios (Ac₂O: free OH) are shown in Table 3. Acetylated hemicelluloses were precipitated and washed in large ethanol bath (40 mL) three times and air dried for overnight.

Fourier Transform Infrared spectroscopy

A Perkin Elmer FTIR, equipped with an ATR cell, was used to collect spectra between 650 cm⁻¹ to 4000 cm⁻¹. Each spectrum were run in duplicate with 16 scans per sample at 2 cm⁻¹ resolution. The Unscrambler X software was used to normalize the spectra, and conduct Principal Component Analysis (PCA) and Partial Least Square (PLS).

Proton Nuclear Magnetic Resonance (¹H-NMR)

A 500 MHz Bruker NMR was used to perform ¹H-NMR analysis. Deuterated DMSO-d₆ was used as the NMR solvent, e.g., 3-4 mg of either xylan or acetylated xylan were added to 600 μL of DMSO-d₆. A drop of trifluoroacetic acid was added to the NMR tube to shift the peak associated with water further down field. All chemical shifts are relative to tetramethylsilane (TMS) at 0 ppm. The degree of substitution was calculated using the below equation (1)

$$\text{DS (Degree of substitution)} = \frac{\text{Integral of CH}_3 \text{ prton} / 3}{\text{Integral of hemicellulose proton} / 6} \text{ eq (1)}$$

Principal Component Analysis (PCA) & Partial Least Square (PLS) statistical analysis

Multivariate tools such as PCA and PLS are commonly used to analyze spectral data and assist with the development of quantitative models for specific properties of interest. They also reduce the amount of sample data, in this case 1675 measurements of NIR spectral intensity, into a few variables with little loss of information. These reduced variables are known as Principle Components, or factors, and are independent or orthogonal to one another. PCA is an undirected analysis, meaning it does not require any additional information about samples and is simply

looking for the greatest sources of variation among input data; in this case the FTIR spectra. In this work PCA was used to evaluate the reproducibility of the FTIR replicates, and conduct initial screening²⁵.

Unlike PCA, PLS is a directed analysis and is commonly used with vibrational spectroscopy to predict some information associated with the chemical features contained in the spectral data, e.g., the chemical composition of a mixture or some physical property such as strength or thermal properties. It requires additional information about the samples obtained by some standard test method and is used to develop a regression model based on the vibrational spectra and the property of interest. This regression model can then be used with the spectra of ‘unknown’ samples to predict the property of interest, usually much more rapidly than the standard method. For the current study, the FTIR spectra were used to predict the acetyl DS of both the soluble and the insoluble hemicellulose samples. In this work, the PLS models were run with full cross validation²⁵⁻²⁶.

Result and discussion

Table 3 summarizes the experimental conditions used for acetylation of the hemicellulose samples. For the soluble samples the resulting DS as measured by solution ¹H-NMR. In theory, an Ac₂O/OH mole ratio of one should produce a DS value of two. However, due to the presence of residual moisture higher, and incomplete reactions, higher concentrations of Ac₂O were required to achieve complete esterification.

Table 3. Experimental condition for all samples. Molar ratio represents the mole ratio between acetic anhydride and free OH. (^a DS value not available due to insolubility of the sample in DMSO, ^b solubility was tested in DMSO, ^c commercially available cellulose).

Sample	Free OH (mmol)	Ac ₂ O (mmol)	Ac ₂ O (μL)	Molar ratio (Ac ₂ O:OH)	DS	Solubility ^b
HW1	1.22	0	0	0	0.00	X

Table 3 (continued).

HW1-MR1.0	1.22	1.22	123	1.0	0.59	O
HW1-MR1.3	1.22	1.62	161	1.3	1.24	O
HW1-MR1.6	1.22	2.04	200	1.6	N/A ^a	X
HW1-MR2.0	1.22	2.44	239	2.0	N/A ^a	X
HW2	1.23	0.00	0	0	0.00	X
HW2-MR0.5	1.23	0.61	66	0.5	0.14	O
HW2-MR0.75	1.23	0.92	95	0.75	0.18	O
HW2-MR1.0	1.23	1.23	124	1	0.55	O
HW2-MR1.3	1.23	1.64	163	1.33	1.12	O
HW2-MR1.5	1.23	1.84	182	1.5	1.18	O
HW2-MR1.6	1.23	2.05	201	1.66	1.54	O
HW2-MR2.0	1.23	2.45	240	2	N/A ^a	X
HW3	1.24	0	0	0	0.00	X
HW3-MR1.0	1.24	1.24	125	1.0	0.72	O
HW3-MR1.3	1.24	1.65	164	1.3	1.30	O
HW3-MR1.6	1.24	2.06	203	1.6	N/A ^a	X
HW3-MR2.0	1.24	2.48	242	2.0	N/A ^a	X
SW1	1.29	0	0	0	0	O
SW1-MR1.3	1.29	1.72	170	1.3	0.91	O
SW1-MR3.0	1.29	3.86	382	3.0	1.92	O
CA ^c	-	-	-	-	1.75	O
CA2 ^c	-	-	-	-	2.55	O
CA3 ^c	-	-	-	-	2.47	O
CA4 ^c	-	-	-	-	2.45	O

Table 3 (continued).

CA5 ^c	-	-	-	-	2.52	O
CA6 ^c	-	-	-	-	2.47	O

Proton Nuclear Magnetic Resonance (NMR)

Proton NMR is a relatively fast, accurate and reliable method for measuring the DS of cellulose esters²⁷. It can also be used to measure the ring substitution patterns for ester groups²⁸⁻²⁹. However, NMR spectrometers are very expensive, and the sample must be soluble to provide high quality data.

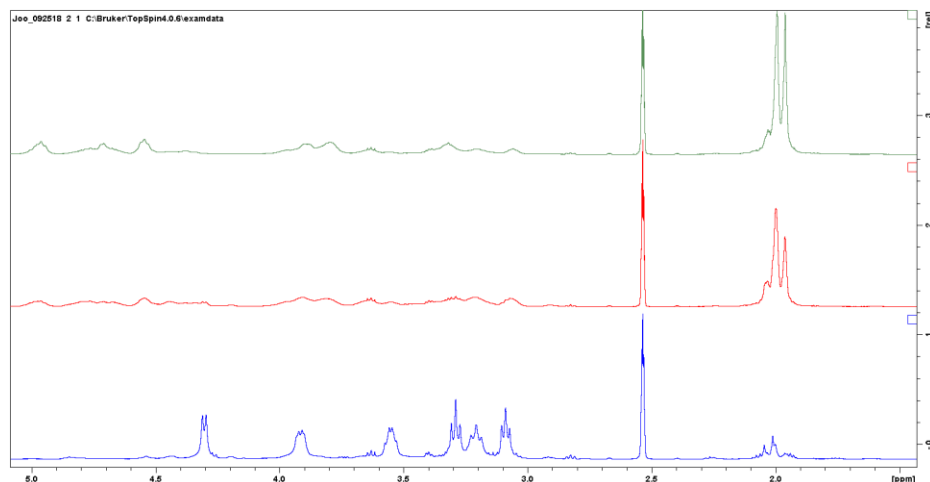


Figure 1. ¹H-NMR spectra of HW2-MR0.75, MR1.3, and MR1.6, from bottom to top. The respected degree of substitution values are 0.18, 1.12, and 1.54.

In this work, ¹H-NMR was used to measure the DS of all the soluble acetylated hemicellulose samples. Representative spectra for a series of partially acetylated HW2 samples are shown in Figure 1. The individual protons were assigned by following the peak assignments developed by Fundador³⁰. The chemical shifts of 4.30, 3.09, 3.29, 3.55, 3.21, and 3.91 ppm represent peaks assigned to H1, H2, H3, H4, H5_{axial}, and H5_{equatorial} respectively, of the xylan starting material. For the acetylated xylans the chemical shifts of 4.71, 4.54, 4.96, 3.78, 3.32, and 3.88 ppm represent peak assignments for H1, H2, H3, H4, H5_{axial}, and H5_{equatorial}, respectively. The protons on the CH₃ of the acetyl group are seen at about 2.0 ppm. For the protons for the

methyl group on the acetyl located at C2 and C3 were seen at 1.99 ppm and 1.96 ppm, respectively²⁹. As expected the calculated DS increases as the Ac₂O to free OH ratio increases. Also, their distinct changes in the chemical shift of the backbone protons as the hydroxyl groups are replaced with acetyl groups.

As the acetyl DS increases there were also significant changes in the solubility of the xylan rich hardwood samples. At DS of 1.5 and above the solubility of the hardwood acetates samples in DMSO decreased dramatically, and gel particles were visible in the NMR tubes. These gel particles persisted even after extensive agitation. While part of the sample dissolved in DMSO there is an obvious question as to whether the ¹H-NMR spectra represent the entire sample. It is also worth noting that cellulose acetates with very high DS, e.g., samples with a DS of 2.9-3.0, are difficult to dissolve, and requires special solvents to obtain truly homogeneous solutions.

Thus, there is a need for an alternative method for measuring the DS of the samples. It is also worth noting that some of the starting hemicelluloses also had solubility challenges. The complex relationship between the structure of hemicelluloses and their DS will be detailed in Chapter 3.

Discussion of characteristic peaks from FTIR-ATR

During the acetylation reaction, the readily available OH groups are being replaced with acetyl group, and these changes can be observed by FTIR as seen qualitatively in Figure 2. The major vibrations in hemicelluloses and acetylated hemicelluloses are detailed in Table 4. Major changes in the FTIR spectra of the acetylated hemicelluloses include: a new peak at 1210 cm⁻¹ that represents C-O stretching within the acetyl group, a new peak at 1380 cm⁻¹ that represents methyl stretch on the acetyl group, and a new peak at 1740 cm⁻¹ peak that represents C=O carbonyl stretch of the acetyl group³¹. As the acetyl DS increases there is a corresponding decrease in the -OH peak at 3400 cm⁻¹ as the acetyl groups replace free hydroxyl groups.

Table 4. List of characteristic peaks for glucan/xylan and acetylated glucan/xylan³¹⁻³².

Wavenumber (cm ⁻¹)	Xylan	Acetylated xylan
900	C ₁ -β-linkage	C ₁ -β-linkage
1030	C-O-C of the glucan/xylan backbone	C-O-C of the glucan/xylan backbone
1160	Glycosidic linkage	Glycosidic linkage
1210	-	C-O stretching of acetyl group
1380	-	CH ₃ stretching of acetyl group
1640	H-O-H bending of absorbed water	H-O-H bending of absorbed water
1740	-	C=O stretch from the acetyl group
3200 - 3500	-OH stretching	-OH stretching of unreacted xylan

Another interesting peak change to note from the Fig 2 is the H₂O bending peak from the absorbed water, 1640 cm⁻¹³¹. Before acetylation the hemicellulose is rich with in free hydroxyl group, therefore there is a significant intensity for this bending vibrations in the unmodified hemicelluloses. As these free hydroxyls are eliminated by the more hydrophobic acetyl groups the adsorbed water bending vibration becomes less evident, e.g., HW2-MR1.3 or essentially disappears for the highly acetylated hemicellulose, e.g., HW2-MR2.0. These n systematic, qualitative changes suggest the opportunity to use FTIR to provide a more rigorous method to measure the DS of hemicellulose acetates.

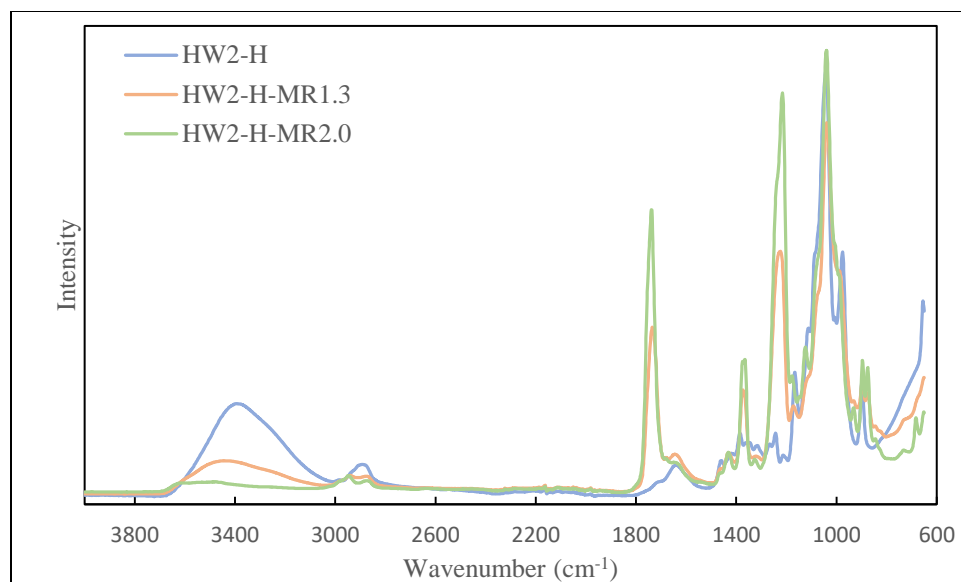


Figure 2. Area normalized ATR-IR of HW2 and acetylated HW2.

Principal Component Analysis

As mentioned above PCA can be viewed as an ‘undirected analysis’ which seeks to identify large differences in the spectral data set. The PCA score plot for the Principal Component 1 (PC1) vs. Principal Component 2 (PC2) is shown in Figure 3. The x-axis is PC-1 and represents 83% of the information contained in the FTIR spectra. The y-axis is PC-2 and represents an additional 10% of the information contained in the FTIR spectra. As expected, there are some clear trends in the results from the PCA analysis of the FTIR spectra. First, on PC-1 all of the unmodified samples are positive relative to the center point, while all highly acetylated samples are negative. These differences explain 83% of the spectral data. At the same time there are some subtle changes, accounting for an additional 10% of the spectral data.

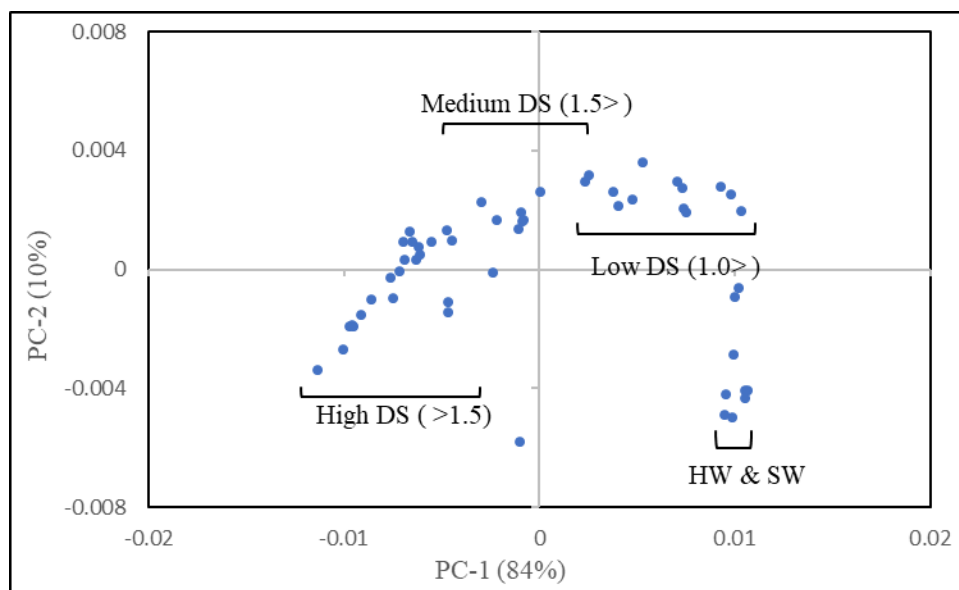


Figure 3. PCA score plots from the FTIR spectra of native and acetylated HW1, HW2, HW3, and SW1 hemicelluloses.

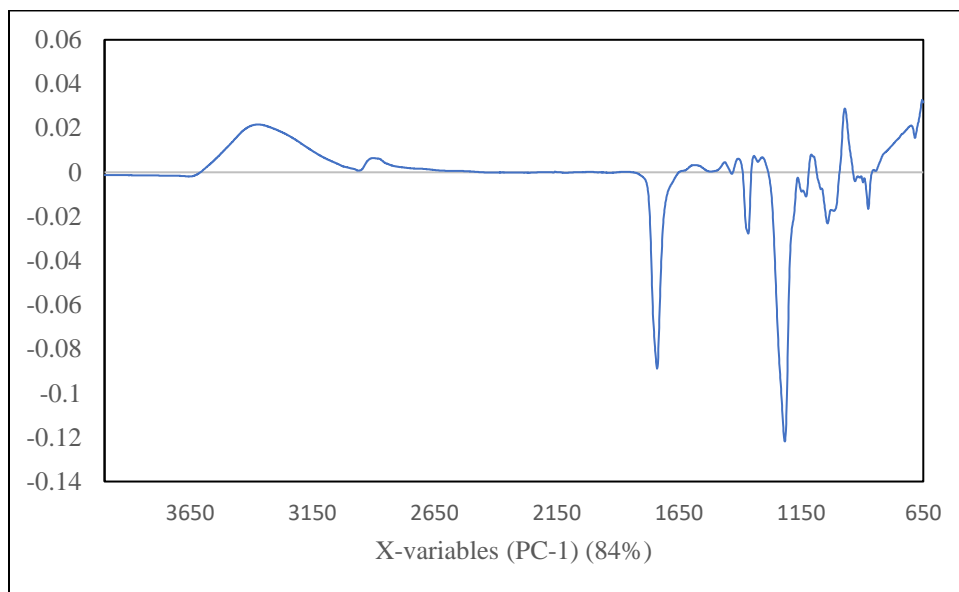


Figure 4. PCA-PC1 loading plots for the samples shown in Figure 3.

The loadings plot in Figure 4 shows the FTIR vibrations that are responsible for the trends seen in Figure 3. This plot reinforces the qualitative differences anticipated from visual inspection of the spectra. Specifically, the loading plots show the samples that are positive along

PC1, e.g. those with a low DS, have higher intensity in the hydroxyl region (3400cm^{-1}) and less intensity in the three acetyl regions, e.g., 1210 cm^{-1} , 1380 cm^{-1} and 1740 cm^{-1} . Samples with a high DS show the opposite trend.

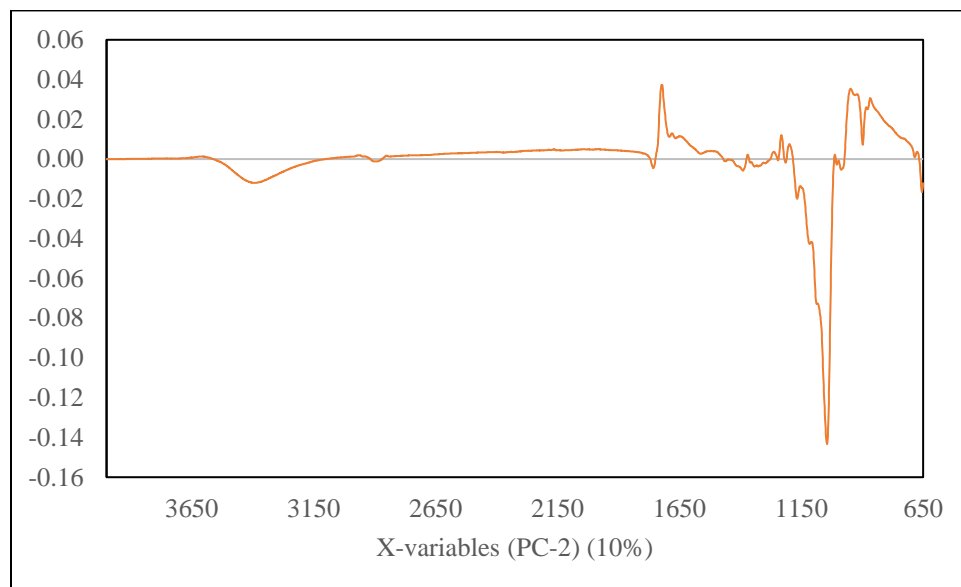


Figure 5. PCA-PC2 loading plots for the samples shown in Figure 3.

Similar to the loading plot of PC1, the loading plot of PC2 from Figure 5 shows the FTIR vibrations that are responsible for the y-axis trend from Figure 3. The second largest variation from the PCA analysis is dominated by the FTIR vibration changes from glucan or xylan backbone region (Table 5). It can be seen from Table 5 that infinitesimal difference in wavenumber is observed when there is only xylan or glucan or mixture of both compounds. Therefore, the variation observed by PC-2 reveals the potential of distinguishing structural difference within hemicellulose.

Table 5. List of glucan and xylan backbone region FTIR vibrations for different compounds³².

Compound	(C-OH), (C-O-C), (C-C), ring				(C ₁ -H), ring		
Arabinan	1141	1097	1070	1039	918	895	807
Arabinogalactan			1074	1045		897	868
Xyloglucan	1153	1118	1078	1041	945	897	
Glucan	1151	1004	1076	1041, 1026	916		840
Arabinoglucuronoxylan + Galactoglucomannan	1161, 1151	1109	1070	1038		898	881

As expected, both the score and loading plots show that the FTIR spectra for this wide range of samples have features that are related to the DS of the samples. It is important to note that the very high DS samples that were insoluble in DMSO and thus do not have ‘known’ DS values are included in the FTIR analysis, and as expected they are highly negative along PC1.

Discussion of partial least squares regression analysis

Along with the FTIR spectra, ¹H-NMR calculated DS information was used to perform partial least square (PLS) analysis to develop a model to predict the DS of the samples. Two different PLS models were developed. The first model was developed using HW1, HW2, HW3, and SW1 native and soluble acetylated samples, while the second, used all the native and soluble acetylated samples from HW1, HW2, HW3, SW1, and CA samples. The purpose of the comparison between two models was to see one if the developed model can predict accurate DS regardless of different backbone structure between xylan and glucan.

The resulting models’ quality can be checked by R² and RMSE (root mean square error) values. RMSE value determines the proximity of the value to the best-fitted line. Both values for each developed model are presented on Table 6. PLS regression analysis had a similar trend of score plot result as PCA score plot, which is Factor 1 showing increasing DS from negative to positive on the x-axis.

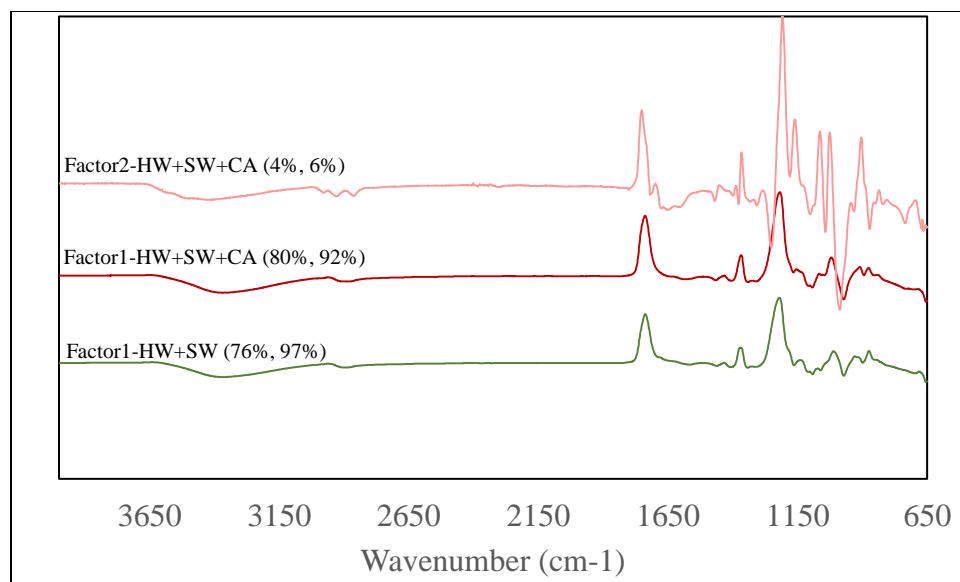


Figure 6. The regression coefficients for all developed models.

PLS factor 1 models

During the PLS model developing stage, it will seek for parameters called regression coefficient to best fit the model²⁶. PLS selects regions that undergo change during the acetylation to use as the regression coefficient (Figure 6). The discovered information from the regression coefficient was similar to PCA. The hydroxyl peak between 3200 – 3500 cm^{-1} decreased as three acetyl characteristic peaks were increasing to represent the progression of acetylation.

Comparing the regression coefficient for HW+SW factor 1 (HS-1) and HW+SW+CA factor 1 (HSC-1), it seems that both PLS models have the same regression coefficient contributing to models. In addition, both factor 1 models use 76% and 80% of the IR spectra information to explain 97% and 92% of the predictions, HS and HSC respectively. This result can conclude that it is possible to expect the same quality of prediction from both models. The factor 2 of the HSC model will be discussed later.

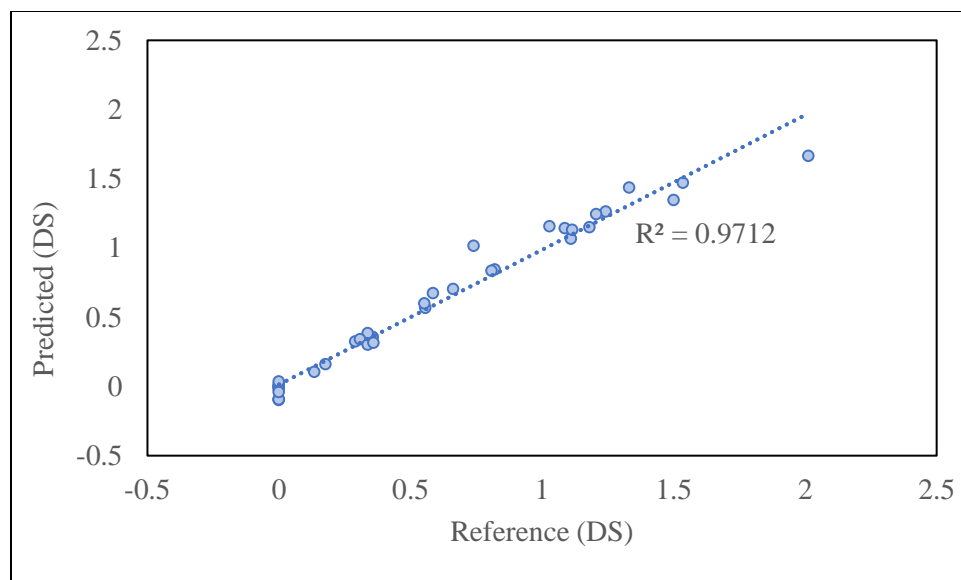


Figure 7. PLS regression result for HW+SW factor 1 (HS-1) model.

The result of the prediction result from Figure 7 seems promising using HS-1 model to predict DS of internal acetylated hardwood and softwood hemicelluloses. The R-squared and RMSE values from Figure 6 confirms a high correlation and a low error on prediction. The prediction of high DS insoluble acetylated HW and SW samples using HS-1 model will be discussed later. Regardless of the similar regression coefficient between HS-1 and HSC-1, the prediction results for HSC-1 was not as successful as the HS-1 model. Figure 8 shows the prediction plot for HSC-1 model. R-squared value of 0.92 does not seem bad. However, focusing on DS 2.5 region for cellulose acetate samples, it was noticed that the prediction results were not accurately close to the calculated DS values. Therefore, further investigation of adding factor 2 to HSC model was pursued.

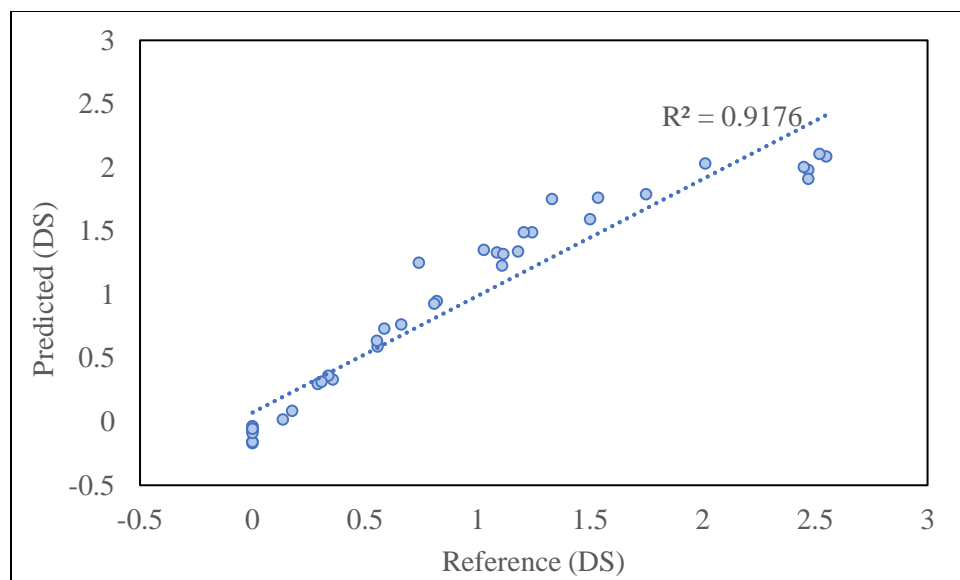


Figure 8. PLS regression result for HW+SW+CA factor 1 (HSC-1) model.

PLS factor 2 model for HW+SW+CA

A different regression coefficient result was discovered for HSC-2 compared to factor 1 of the previous two models from Figure 6. This difference is rooted from different chemical nature between cellulose acetate and hemicellulose acetate that leads to a slight shift in wavenumber for all vibration bands. In the “fingerprint” region between 900 and 1170 cm^{-1} , there are four sharp peaks from the right that refer to anomeric carbon to the beta linkage, C-H and C-O linkage in the backbone, and glycosidic linkage. Due to the small shift in wavenumber between cellulose acetate and hemicellulose acetates, the shift in fingerprint region is more sensitive to cellulose acetate backbone than hemicellulose acetate backbone, a slight shift of FTIR vibration was found on Table 5. And, the other three major acetyl characteristic vibrations match well for both cellulose and hemicellulose acetates.

With the additional use of spectral information, the resulting DS prediction improved as can be seen on Figure 9. The R-squared and RMSE improved, and the prediction for 2.5 DS region is in the linear region again.

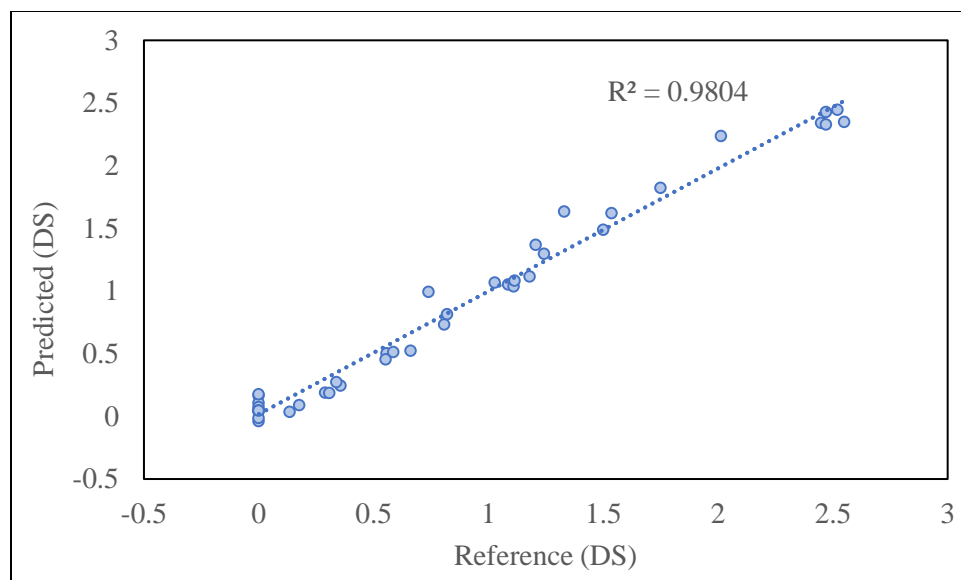


Figure 9. PLS regression result for HW+SW+CA factor 2 (HSC-2) model.

Table 6. List of R-squared and RMSE value for all three models.

PLS model	Factor	Abbreviation	R ²	RMSE
HW+SW	1	HS-1	0.97	0.10
HW+SW+CA	1	HSC-1	0.92	0.24
HW+SW+CA	2	HSC-2	0.98	0.11

Prediction results of developed PLS models

Now that HS-1, HSC-1, and HSC-2 models have been developed, these models can be used to predict the DS of both soluble and insoluble samples. The prediction results can be found on Figure 10, Figure 11, and Figure 12. For each graph, reference plot represents the calculated DS. As anticipated from the PLS regression result the prediction result was satisfactory for HS-1 model. Low to medium DS matched accurately with reference, and insoluble samples from hardwoods and softwood resulted in logical outputs. All insoluble samples had predicted DS values higher than soluble DS, e.g., MR2.0 showed higher prediction compared to MR1.6. However, due to lack of sample with DS above 2.0, the prediction quality of cellulose acetate samples were poor.

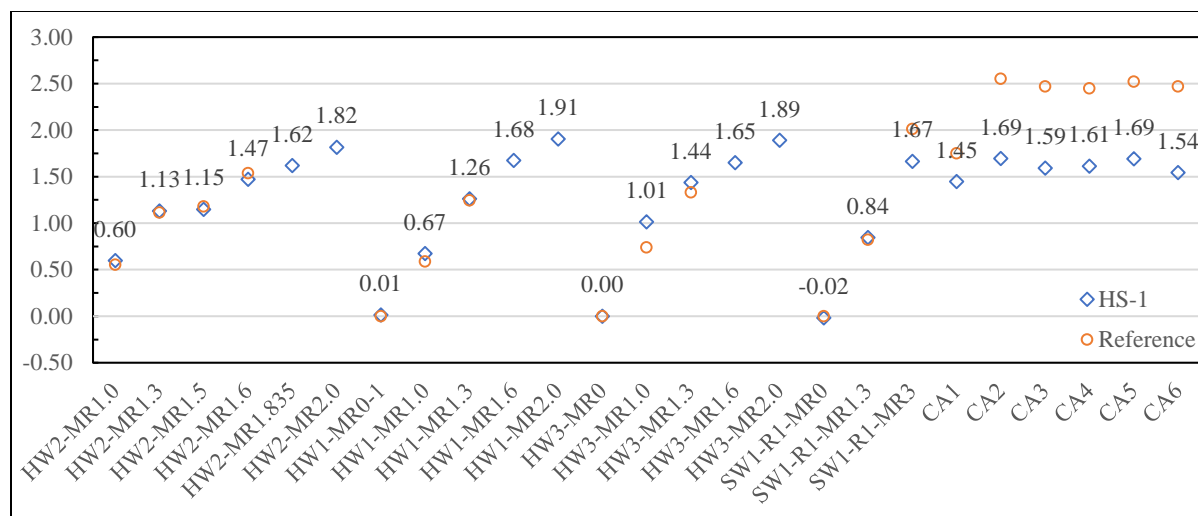


Figure 10. Prediction result using HS-1 model.

Adding cellulose acetate samples from the previous model, HSC-1 predictions are shown from the below figure. The prediction results for cellulose acetates improved compared to HS-1, but the predictions are not as close enough to reference values to provide a satisfying result. And, other HW and SW acetylated hemicelluloses predictions have been overestimated. Theoretical max DS for HW and SW are 2.0 and 2.3, however, prediction results were higher than 2.0 for hardwood samples. The overestimation is due to the stronger regression coefficient for HSC-1 for acetyl vibrations compared to HS-1.

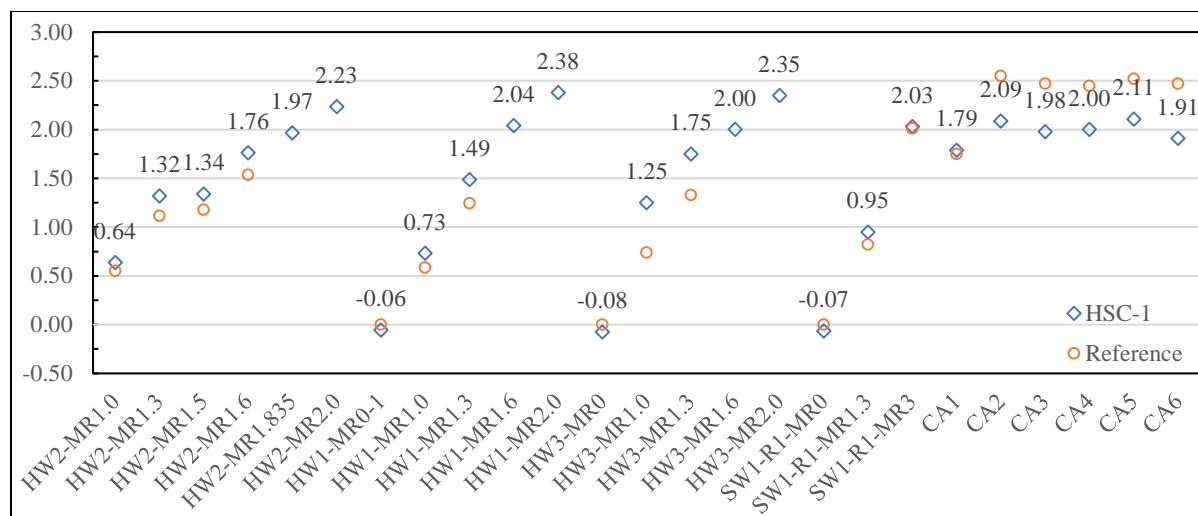


Figure 11. Prediction result using HSC-1 model.

In order to improve the prediction for cellulose acetate samples, regression coefficient factor 2 was added in addition to HSC-1. The conclusion of the two factor model provided more accurate DS predictions for cellulose acetate samples. However, the issue of overestimation of hemicellulose acetates sample remained. The additional regression coefficient factor amplified the effect of both acetyl and backbone vibrations for cellulose acetate, but only the acetyl coefficient was amplified for hemicellulose acetate because of the backbone difference between cellulose acetate and hemicellulose acetate. As of result, cellulose acetate samples were able to reach better DS prediction with factor 2 but, hemicellulose acetate samples overestimated DS due to an extended implication of two coefficients for acetyl vibrations.

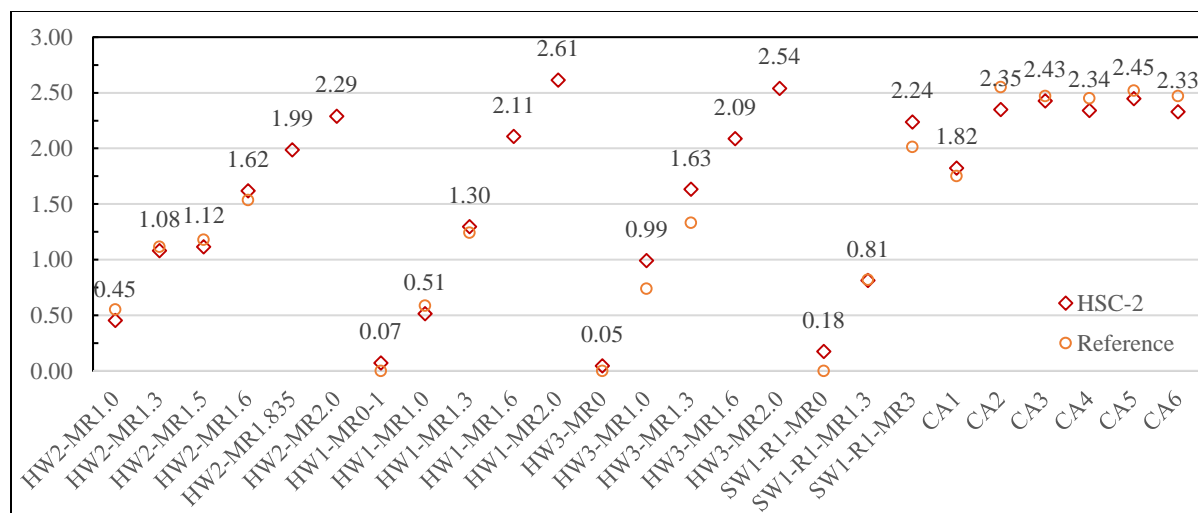


Figure 12. Prediction result using HSC-2 model.

Conclusion

The solubility of hemicellulose acetates is a complex function of the acetyl DS, and the structure of the starting hemicellulose. Acetylation of residual hemicelluloses could be effectively achieved using [DBNH][OAc] as the solvent and Ac₂O. FTIR and ¹H-NMR analysis were conducted to obtain information on the extent of the reaction for different hemicellulose acetates. The lack of solubility for the xylan rich hardwood hemicelluloses at high DS limited their analysis with the traditional ¹H-NMR tools. Thus, the FTIR spectra for hemicellulose samples with a wide range of DS values were used to construction PLS models that could be used to predict the DS on all the samples, soluble or insoluble. then multivariate analysis of PCA and PLS was examined in order to predict the DS of insoluble acetylated hemicelluloses. The results of PCA and PLS were satisfactory due to high R² and RMSE obtained values of 0.98 and 0.07 respectively from the developed regression model. Also, the prediction results were accurate for the samples made from HW1, HW2, and HW3, however, there was observed discrepancy when hemicellulose based PLS model (HS-1) was attempted to predict DS of cellulose acetates. This discrepancy may be due to the compositional difference between hemicelluloses and cellulose. This difference can limit the extend use of the regression model to predict the DS but, as long as the sample of interest is enriched with hemicellulose composition then, the prediction results are in the trustworthy region. And, HSC-2 model which has

incorporated cellulose acetates resulted in predictions that shows highly accurate prediction for cellulose acetates. But, the former model resulted in overestimated DS for hemicellulose samples. Therefore, two developed models can be used to predict DS of hemicellulose samples or cellulose acetate samples. In addition to the predictability of the model, being able to obtain DS information only by using ATR-IR can save a tremendous amount of analyzing and sample preparing time and the method is versatile when compared to titration or NMR method.

Chapter 3: Crystallography study of hemicellulose and related solubility

Introduction

Hemicelluloses are the second most abundant carbohydrate found in nature³³. Depending on the plant, it can be comprised of 20 to 30 % of a plant's cell wall³⁴. Its four main building block monomers are arabinose, xylose, mannose, and galactose. The ratio of these four monomers varies with the biomass source, and can be heavily impacted by the process used to isolate the hemicellulose. Some hemicelluloses also contain varying amounts of side groups such as 4-O-methyl glucuronic acid, and acetyl substituents³⁵. Due to its complex structure and intimate relationship with cellulose and lignin, it is extraordinarily difficult to selectively remove hemicellulose from biomass. Commercial pulping tends to remove hemicelluloses along with the lignin³⁶, although more lignin is commonly removed. Depending on the pulping conditions the hemicellulose's structure will change significantly, commonly with a loss of liable side groups, and an overall decrease in molecular weight (MW)⁸.

There are several general methods used to remove hemicelluloses from biomass, water-soluble, alkaline, and acidic extractions^{35, 37}. Each extraction methods has an effect on both the isolated hemicellulose, and also the residual hemicellulose left in the 'biomass'. The type of biomass, e.g., angiosperms, gymnosperms, and the anatomical fraction, e.g., stems, leaves, bark, branches, and even the age of the plant can all have a role in the chemical structure of the hemicellulose, and the effectiveness of different hemicellulose isolations methods. For example, simple hot-water extraction of ryegrass leaves produces a moderate MW (~20,000 g/mol) galactoarabinoxylan fraction, and noticeable amounts of pectins. Mild alkaline extraction provides high MW (~30,000 g/mol) galactoarabinoxylans with glucuronic acid side groups, while even more alkaline solutions will cleave off most of the acid groups from the xylans³⁷. Using dilute acid extraction method on hardwood can dissolve hemicelluloses, and the dissolved hemicelluloses can further hydrolyze and create a variety of byproducts³⁵.

Even with numerous laboratory and commercial methods for separating hemicelluloses from biomass, it remains a challenge to produce a cellulose pulp that is completely free of

hemicellulose. This has great commercial importance since high purity cellulose, so called dissolving pulps, are a value-added product and growing market demand. The residual hemicelluloses in these dissolving pulps can have a negative impact on the resulting final product, especially when the product requires some sort of intermediate dissolution step^{5,7}. In the case of commercial cellulose ester products, the undissolved hemicellulose ester ‘gel’ particles must be removed by an expensive filtration process³⁸. Previous work has used centrifugation to isolate these gel particles, and subsequent characterization shows they are xylan^{5-7,9}. Additional studies of isolated xylan acetates have shown their limited solubility in a number of different solvents^{22,39}.

In addition to their solution properties, the solid-state properties of xylan acetates have been studied. Thermal properties using TGA and DSC were studied and the properties were compared to native xylan²⁸. Thermal degradation temperature for xylan acetate (335 °C) higher than native xylan (283 °C). Both native and xylan acetate (DS=2.0) have a subtle glass transition that is difficult to observe, while xylan acetate with DS of 1.2 had a distinct glass transition temperature between 160 and 200 °C.

Therefore, this study focused on better understanding the relationship between hemicellulose composition, the degree of substitution (DS) and the ordering of hemicellulose acetates. Hemicelluloses were extracted from hardwood and softwood dissolving pulps, and then acetylated to different DS levels, and their ordering and solubility were measured.

Experiment methods and materials

Commercial hardwood and softwood pulps were used for this study and their general characteristics are listed on Table 7. Conventional kraft pulping alone is insufficient to remove enough hemicellulose to produce high quality, dissolving pulps, therefore additional unit operations are needed. One common operation is known as prehydrolysis Kraft pulping (PHK), where the chips are treated with one of two alternative processes, 1) direct steaming at temperatures between 160 and 180 °C for between 30 min and 3 hours, or 2) treatment with dilute mineral acid (0.3-0.5% H₂SO₄) at temperatures between 120 and 140 °C²⁰. This treatment

can create organic acids, which can also contribute to the hydrolysis of the hemicelluloses, and increase their solubility. A second common commercial process is cold-caustic extraction (CCE). The conditions for CCE treatment include mixing the pulp with a solution of 5-10% NaOH for at least 10 minutes at temperatures between 25 and 45 °C²⁰. Finally, the acid sulfite (AS) pulping process is commonly conducted under strongly acidic condition, e.g., pH between 1.5 and 2, and the pulping temperature ranges from 125-145 °C for cooking times up to 7 hours²¹. All samples used in the work were commercial dissolving pulp graciously provided by Eastman Chemical Co. All chemicals were purchased from Fisher Scientific or Sigma Aldrich, and used without further purifications.

Extraction of hemicellulose from dissolving pulps

The hardwood (HW) PHK hemicellulose samples were recovered from a commercial dissolving pulp process using cold caustic extraction prior to the Kraft pulping. The softwood (SW) hemicellulose was isolated from an AS dissolving pulp in our laboratory using 24% KOH extraction protocol developed by Gardner and Chang⁹. The extraction process is detailed in Lee, et al., 2019, but a brief description is provided here. The commercial dissolving pulp was extracted with 24 wt% KOH solution with 0.5 wt% of sodium borohydride at room temperature for six hours on automatic shaker; the hemicellulose solution was centrifuged washed with ethanol and acetic acid, and precipitated overnight^{10, 22}.

Composition analysis of extracted hemicelluloses

The NREL standard method²³ was used to measure the sugar content of the two hemicellulose samples and the results are shown in Table 7. Composition analysis result for the hemicelluloses.

Table 7. Composition analysis result for the hemicelluloses.

<i>Sample</i>		<i>Composition analysis</i>		
		Glucose (%)	Xylose (%)	Mannose (%)
HW	CCE/PHK	2.1	94.8	0
SW	AS	15.4	53.6	11.4

Synthesis of ionic liquid

Acetylation of the hemicelluloses was conducted using an ionic liquid (IL) as a solvent. The IL was synthesized by mixing equimolar of 1,5-Diazabicyclo[4.3.]non-5-ene (DBN) and acetic acid²⁴. The reaction vial was flushed with nitrogen gas and sealed, and maintained in an ice water bath to control the temperature²⁴.

Dissolution and acetylation of hemicellulose

Hemicellulose was dissolved in IL at 5 wt% for 2 hr at 80°C. The acetylation reaction was initiated by adding acetic anhydride. The amount of acetic anhydride was varied to control the desired DS. Table 8. Experimental condition for hemicelluloses. Molar ratio represents the mole ratio between acetic anhydride and free OH. (^a sample was insoluble in DMSO so the DS was predicted using FTIR (CH 2), ^b glycosidic linkage analysis was only conducted for unacetylated hemicelluloses, ^c solubility was tested in DMSO, ^d solubility was tested in water) displays the list amount of acetic anhydride used to target certain levels of DS. Acetylated hemicellulose was precipitated in excess ethanol and washed three more times with ethanol. Finally, it was air dried for overnight.

Fourier Transform Infrared spectroscopy (FTIR)

A Perkin Elmer FTIR, equipped with an ATR cell, was used to collect spectra between 650 cm⁻¹ to 4000 cm⁻¹. Each spectra was run in duplicated with 16 scans per sample at 2cm⁻¹ resolution.

Proton Nuclear Magnetic Resonance (¹H-NMR)

A 500 MHz Bruker NMR was used to perform ¹H-NMR experiment. Deuterated DMSO-d₆ was used as the NMR solvent, e.g., 3-4 mg of either xylan or acetylated xylan were added to 600 μL of DMSO-d₆. A drop of trifluoroacetic acid was added to the NMR tube to shift the peak associated with water further down field. All chemical shifts are relative to tetramethylsilane (TMS) at 0 ppm. The DS was calculated using the below equation (1).

$$DS = \frac{\text{Integral of } CH_3 \text{ proton} / 3}{\text{Integral of carbohydrate proton} / 6} \text{ eq (1)}$$

X-ray Diffraction Analysis

The X-ray diffraction patterns were measured with a SmartLab X-ray diffractometer (Rigaku, Woodlands, TX). Operating voltage was 40 kV, and the operating current was 44 mA. A Cu Ka X-ray tube was used to produce X-rays at 0.1541 nm wavelength. Either sample was placed on a quartz sample holder. Measurement of the 2θ angle range from 9° to 41°. Each step was 0.05° and the X-ray detector remained constant for 0.4 s at each step to collect the diffracted X-rays.

Glycosidic linkage analysis

This analysis was conducted to measure the number of glucuronic acid side group present along the HW xylan chain and the monosaccharide composition of the SW hemicellulose. Detail of the glycosidic linkage analysis can be found in Kim, et al., 2018¹⁰. Briefly, the extracted hemicellulose undergoes series of reduction, permethylation, and acetylation to hydrolyze down to partially methylated, alditol acetates (PMAAs). The mixed PMAA products were identified by GC-MS, and analyzed quantitatively by GC-FID with high polar SGE BPX-70 column (25m x 22 μm inner diameter, 0.25 μm thickness). Chromatographic conditions followed the report by Pettolino⁴⁰.

Solubility visual inspection

A visual inspection parameter was developed to semi-quantitatively differentiate between the samples. The numerical scale was used to determine the solubility. A 3 to 4 mg sample was added to 600 μ L of solvent (DMSO or water) in a closed vial. The sample was placed in an ultrasonic water bath held at 40 °C for one minute, and then set on a table overnight to complete the dissolution or allow for sedimentation of undissolved particles. A visual inspection score between 1 and 3 was assigned. The score of 1 represents obviously insoluble with insoluble sediments and solution was cloudy, a score of 2 represents partial solubilization, some amounts of sediments but the solution was clear, and a score of 3 represents completely soluble, no sediments and a clear solution.

Result and discussion

Table 8. Experimental condition for hemicelluloses. Molar ratio represents the mole ratio between acetic anhydride and free OH. (^a sample was insoluble in DMSO so the DS was predicted using FTIR (CH 2), ^b glycosidic linkage analysis was only conducted for unacetylated hemicelluloses, ^c solubility was tested in DMSO, ^d solubility was tested in water) summarizes the amount of acetic anhydride used to initiate the acetylation reaction and resulting acetyl DS. The actual stoichiometry is difficult to measure due to the presence side groups on the HW xylan and glucose and mannose, with their three hydroxyl groups on the SW hemicellulose, and also residual moisture.

The solubility results for the partially acetylated hemicelluloses are shown in Table 8. Experimental condition for hemicelluloses. Molar ratio represents the mole ratio between acetic anhydride and free OH. (^a sample was insoluble in DMSO so the DS was predicted using FTIR (CH 2), ^b glycosidic linkage analysis was only conducted for unacetylated hemicelluloses, ^c solubility was tested in DMSO, ^d solubility was tested in water). Both the partially acetylated HW and SW hemicelluloses were soluble in DMSO. The fully acetylated SW hemicellulose was partially soluble in DMSO, while the HW hemicellulose was essentially insoluble. Unacetylated hemicelluloses were both partially soluble in DMSO however, SW hemicellulose completely

solubilized in water when HW hemicellulose did not dissolve and formed a turbid solution with sediment

The result of glycosidic linkage analysis from GC-MS and GC-FID shows the absence of glucuronic acid side unit on HW hemicellulose and mole ratio between glucuronic acid and xylan of 1: 6.9 for SW hemicellulose. This is consistent with prior work by Wilson⁸ that showed kraft pulping was capable of cleaving glucuronic acid, while acid sulfite pulping retained glucuronic acid branch points.

These results are consistent with the behavior of cellulose esters where the cellulose starting material is insoluble on most common solvents, while commercial cellulose esters with an intermediate DS (DS 1.8-2.5) are soluble in a wide variety of organic solvents. However, cellulose acetates with a very high DS, greater than 2.85, are not soluble in most organic solvents.

Table 8. Experimental condition for hemicelluloses. Molar ratio represents the mole ratio between acetic anhydride and free OH. (^a sample was insoluble in DMSO so the DS was predicted using FTIR (CH 2), ^b glycosidic linkage analysis was only conducted for unacetylated hemicelluloses, ^c solubility was tested in DMSO, ^d solubility was tested in water)

Sample	Free OH (mmol)	Ac ₂ O (mmol)	Ac ₂ O (μL)	Molar ratio (AA:OH)	DS	GlucA:Xyl (mole ratio)	Solubility
HW	1.2	0	0	0	0	0	1 ^d
HW- MR1.3	1.2	1.6	163	1.3	1.1	N/A ^b	3 ^c
HW- MR2.0	1.2	2.5	240	2	1.9 ^a	N/A ^b	1 ^c
SW	1.3	0	0	0	0	1:6.9	3 ^d
SW- MR2.0	1.3	2.6	251	2	1.9	N/A ^b	2 ^c

Characterization of acetylation reaction by FTIR and ¹H-NMR

As we reported in our prior work (Lee, et al., 2019) FTIR and ¹H-NMR were used to characterize the starting materials and acetylated hemicelluloses. Representative FTIR spectra

are shown in Figure 13 and corresponding IR peak assignments are shown in Table 1. The unacetylated samples are missing all the common acetyl vibrations (1210 cm^{-1} , 1318 cm^{-1} , 1740 cm^{-1}). While the acetylated samples, HWMR1.3, HW-MR2.0, and SW-MR2.0, have reduced intensity in the hydroxyl vibration at $3200\text{--}3500\text{ cm}^{-1}$ and appearances of C=O (1210 cm^{-1}), -C-CH₃ (1318 cm^{-1}) and -C-O-C (1740 cm^{-1}) acetyl characteristic peaks. Using Partial Least Squares (PLS) regression the FTIR spectra can be used to quantify the DS of all the hemicellulose samples. As expected increasing the molar ratio of acetic anhydride to hemicellulose hydroxyl groups increased the DS of the samples.

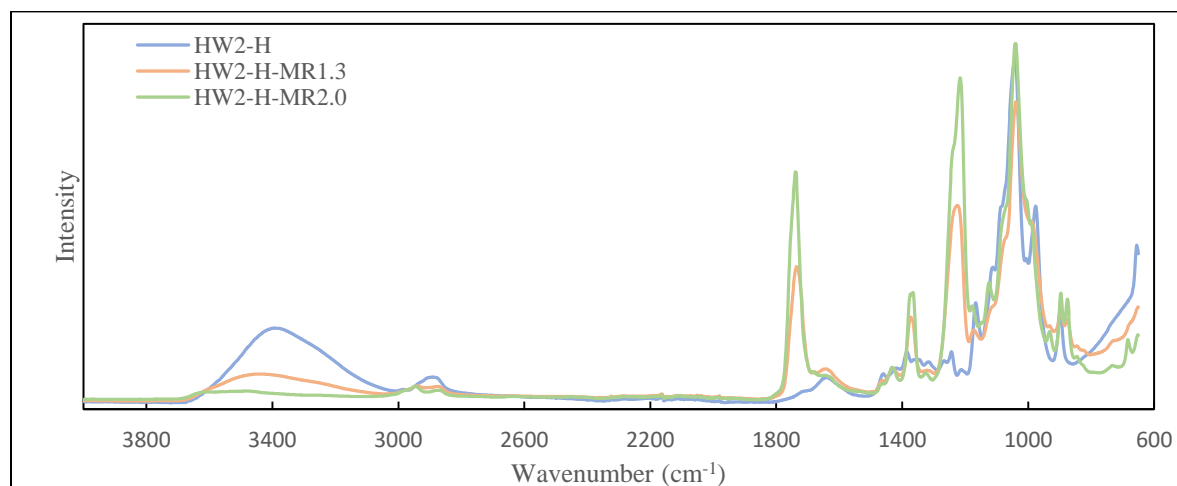


Figure 13. FTIR spectra for HW at different DS.

The DS of the soluble samples was also measured with ¹H-NMR allowed accurate quantitative calculation of DS. Proton peaks from 3.0 ppm to 5.2 ppm refer to carbohydrate ring protons. In addition, Figure 15. H-NMR spectra of SW in DMSO-d₆ shows the presence proton of C₁ and O₄-methyl proton peaks from glucuronic acid at 5.1 ppm and 3.4 ppm, respectively, for softwood hemicellulose. The presence of two glucuronic characteristic peaks confirmed the glycosidic linkage analysis. Figure 14. H-NMR spectra of a) HW and b) HW-MR1.3 in DMSO-d₆ shows the methyl proton peaks from acetyl group near 2.0 ppm region for acetylated hemicellulose.

The acetyl DS can be calculated using equation 1. An integral of methyl proton was divided by three because of three protons exist per acetyl group, and an integral of carbohydrate proton was divided by six because there are six protons in xylan backbone, which is the dominant monomer in both hemicelluloses. Only the samples that were completely soluble in DMSO were measured by $^1\text{H-NMR}$.

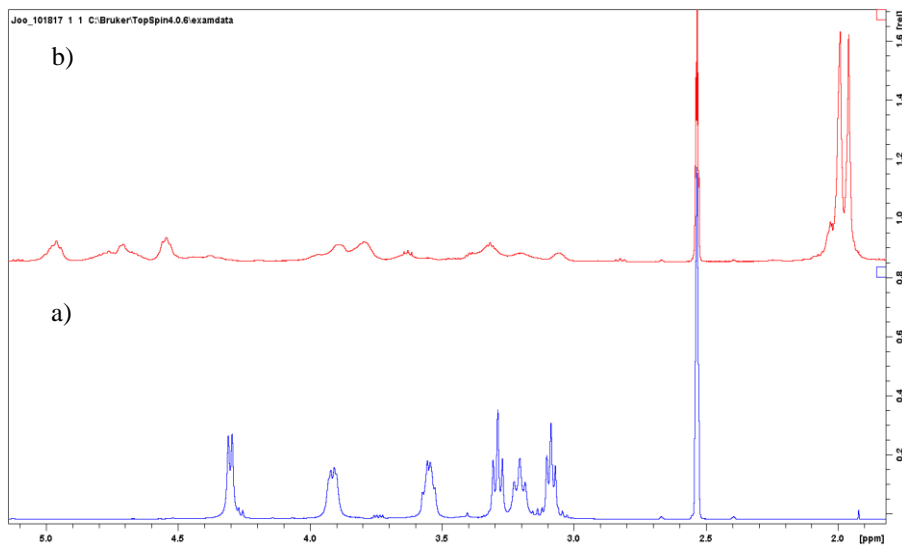


Figure 14. $^1\text{H-NMR}$ spectra of a) HW and b) HW-MR1.3 in DMSO-d_6 .

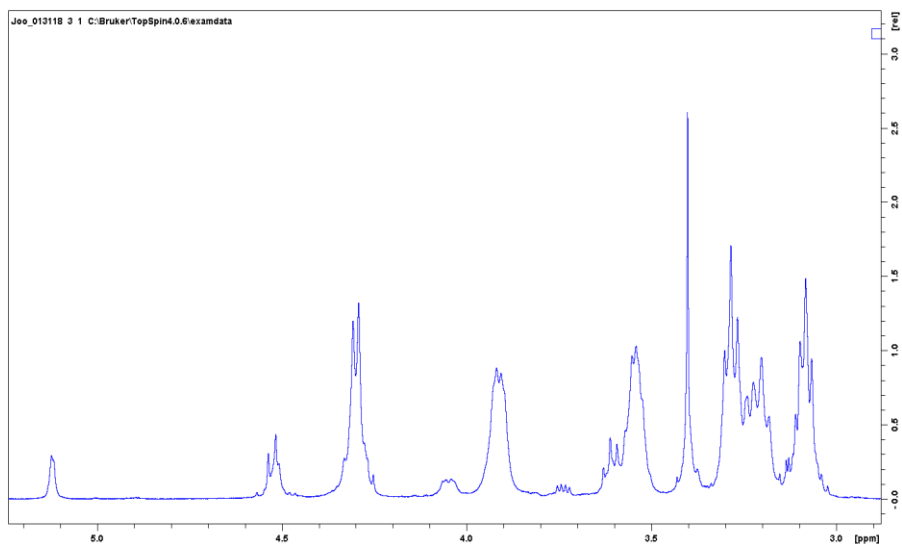


Figure 15. $^1\text{H-NMR}$ spectra of SW in DMSO-d_6 .

Discussion of insolubility of hemicellulose

The solubility of unacetylated, partially acetylated, and fully acetylated hemicellulose varied depending on the source of the hemicellulose, and also their DS. The previous work done by Wilson⁸ described how the structure of SW hemicellulose changed depending on the pulping conditions. During PHK pulping, there is an initial acidic prehydrolysis step followed by the alkaline pulping kraft process. Under acidic conditions, acid-labile arabinose side group was cleaved off, while under alkaline conditions, alkali-labile 4-O-methyl-glucuronic acid side group was cleaved off. Thus, the HW hemicellulose recovered from the commercial PHK process is a linear chain rich in xylan, while the SW hemicellulose produced by AS retained a significant amount of glucuronic acid side groups, (Table 8) and also have a higher percentage of nonxylan monosaccharide units in the backbone.

X-ray diffraction of hemicellulose and acetylated hemicellulose

The crystallinity of cellulose has been extensively studied, and is affected by the source of the cellulose, and the treatment (or lack thereof) used in isolating the cellulose⁴¹. The crystallinity of other carbohydrates is less well-known in large part because they tend to be amorphous, or poorly crystalline, and very dependent on the process used to isolate them⁴².

X-ray diffraction is commonly used to characterize the crystalline properties of cellulose and other carbohydrates. While XRD may be best viewed as providing a ‘relative’ measure of carbohydrate crystallinity, it nevertheless, has great value for providing insights into the solid-state properties of a wide variety of carbohydrates. Cellulose acetates, and other cellulose esters, have been the subject of many studies on the relationship between crystallinity measured with XRD and solid-state properties. In this work, XRD was used to study the properties of the isolated wood hemicelluloses and acetylated hemicellulose.

The XRD patterns for the isolation hemicellulose and their acetylated derivatives are shown in Figure 16 and Figure 17. The XRD pattern for the HW hemicellulose shows a significant amount of order, with well-defined peaks at 2-theta of 19.7° and two smaller peaks at 2-theta of 11.25° and 12.7°. However, HW xylan acetylated to a DS of 1.1 shows only a poorly defined peak centered around a 2-theta of 19.8°. While the full acetylated HW xylan shows small crystalline peaks at 2-theta of 11.9°, 14.5°, 17.5°, and 22.2°.

These changes in the XRD patterns are consistent with the changes seen in cellulose acetates. Before acetylation, the HW xylan had high and well-defined crystalline peaks (Figure 16) consistent with a relatively 'pure' xylan backbone and few glucuronic acid side groups. With the initial acetylation (DS = 1.1) these acetyl side groups are bulky enough to interrupt the well-ordered xylan structure, as seen by a single broad XRD peak.⁴³⁻⁴⁴ (Figure 16). With complete acetylation, the HW xylan behaves like a uniform homopolymer, and shows well ordered XRD pattern. As expected the XRD reflections are very different for the starting HW xylan and the fully acetylated HW xylan⁴³.

Comparing the XRD peaks height and width between HW and HW-MR2.0 suggests that the highly acetylated hemicellulose has a smaller size of crystalline than native hemicellulose.

Similar to hemicellulose, cellulose and acetylated cellulose have a similar change in XRD pattern. Cellulose in native form has a distinctive crystalline peak⁴¹. Cellulose diacetate with DS values between 2.0-2.5, which is equivalent to HW-MR1.3, resulted in halo amorphous shape⁴⁵. Cellulose triacetate with DS value between 2.8-3.0, which is equivalent to HW-MR2.0, resulted in similar crystalline structure again⁴⁵⁻⁴⁶.

Both the native and highly acetylated SW hemicelluloses resulted in amorphous structure (Figure 17). The native SW lacks crystalline peak due to the presence of glucuronic acid side groups, and also the presence of mannose and galactose sugar units in the backbone. As shown in Table 8 only 60 % of the SW hemicellulose is xylose. Both on these features limit the ability of the SW hemicellulose to form well-ordered structures. This observation is consistent with work by Horio's¹¹ where he observed well-defined crystalline peaks for xylan with low amounts of glucuronic acid side groups, and observed amorphous halo xylans that had high levels of glucuronic acid side groups. Fully acetylated SW hemicellulose did not result in crystalline structures since the heterogeneity in the backbone is still a factor, and the glucuronic acid groups are much larger than an acetyl group, and will not pack into an acetyl lattice cell position.

In order to obtain a crystalline structure, it is important for the hemicellulose to have few side groups and a high concentration of a single monosaccharide unit. This work suggests that a xylan rich hemicellulose can accommodate at least 10% of a second monosaccharide. When fully acetylated, uniform hemicellulose can form crystalline structures, although as expected these are very different than the unit cell of the starting hemicellulose.

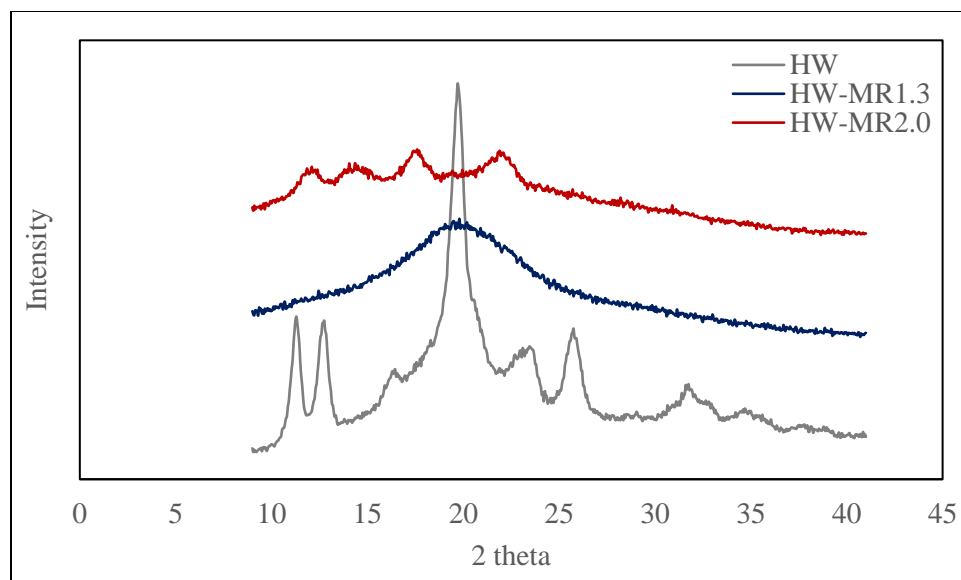


Figure 16. X-ray diffraction graph for the native and acetylated HW samples.

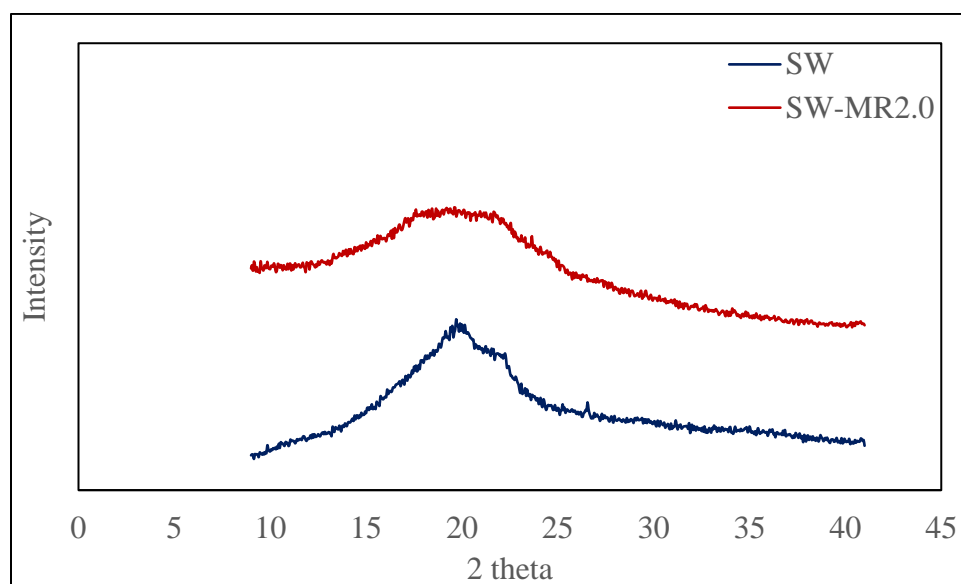


Figure 17. X-ray diffraction for the native and acetylated SW samples.

Discussion of solubility and crystallinity of hemicellulose

It is important to highlight the relationship between crystallinity and solubility of hemicelluloses. Comparing the solubility visual inspection score and XRD results, it appears that

the two amorphous samples (SW and HW-MR1.3) were completely soluble, and the amorphous SW-MR2.0, was partly soluble. The two highly crystalline samples (HW and HW-MR2.0) were insoluble.

The amorphous SW hemicellulose was soluble in water but the crystalline HW hemicellulose was not. Previous work by Andrewartha⁴⁷ rationalized xylan solubility by noting that inter-chain aggregation was limited by arabinose side unit. For arabinoxylan hemicellulose, the presence of arabinose side group can prevent the inter-chain interaction with another chain of unsubstituted xylan by increasing aggregate stability. Thus, xylan with a high amount of arabinose resulted in better solubility than xylan with a very low amount of arabinose. Similarly, HW1-H has substantial amount of xylan, 94.8%, and the absent of side groups due to the consequence of pulping conditions described previously.

Unlike the HW hemicellulose, the SW hemicellulose has a relatively high frequency of glucuronic acid group, e.g., approximately one every 7 xylan repeat units, which will limit inter-chain interactions.

In addition to being a bulky group that limits chain packing, the carboxylic acid on the glucuronic acid is negatively charged, and high levels of the carboxylic acids will create repulsion effects between the chains and further prevent chain aggregation. The importance of this charge stability was also studied by Linder 2003⁴⁸. It was observed that the presence of an electrolyte (1 mM NaCl) in xylan solution decreased the xylan aggregate stability and caused sedimentation of xylan.

The relationship between higher levels of crystalline and poor solubility is expected. In ordered, tightly packed chains, there is limited opportunity for solvation to occur between solute and a solvent. In addition, the positive polymer-solvent interactions must overcome the lower energy structures present in the crystalline domain. Conversely, amorphous structures provide more opportunity for the solvent molecules to interact with the polymer chains, without having to overcome the crystalline ordering.

Conclusion

Two different kinds of hemicelluloses were used for this study to examine the relationship between hemicellulose structure, solubility and crystallinity. HW has 95% xylan and no significant level of glucuronic acid side groups, which allows for formation of crystalline domains and limits solubility. Conversely, the SW hemicellulose has only 54% xylan in the backbone, and also has a significant amount of 4-O-methyl glucuronic acid side groups. In the non-acetylated samples these differences are manifest with the formation of highly crystalline domains and poor solubility for the HW, and amorphous morphology and better solubility in the SW hemicellulose. The SW dissolved well in water while HW did not

Acetylation of these two hemicellulose added a secondary factor. Partial acetylation of the HW hemicellulose (HW-MR1.3) produced a disordered and soluble material. Complete acetylation (HW-MR2.0 and SW-MR2.0) produced two different effects. Complete acetylation of the HW hemicellulose, with its relatively uniform structure, allowed for the formation of crystalline domains, and a decrease in solubility. Complete acetylation of the SW hemicellulose does not mitigate the heterogeneous nature of the backbone and the presence of the glucuronic acid side groups. These two features continue to dominate the solubility and ordering of the SW hemicellulose.

Chapter 4: Dynamic light scattering study of cellulose acetate in acetone solution

Introduction

Theory of dynamic light scattering (DLS)

Dynamic light scattering measures fluctuation of scattered light by a solute moving through a solvent as a result of random Brownian motion. The scattered light information undergoes mathematical correlation to provide an output value of hydrodynamic particle size. The details of each step in this process are reported below.

A solute diffusing through a solvent is constantly in random motion due to the Brownian motion. This random motion is derived from a constant random collision between the solute and the solvent. And, the movement of the solute is related to the size, or molecular weight (MW), of the particle. There are a couple of factors that can affect the diffusion speed of the particle. First, the size of the particle can affect the speed of diffusion, larger particle size will diffuse slower and smaller particle size will diffuse faster. Second, the viscosity of the solvent is important. Viscosity is the measure of the resistance of the motion of a fluid, therefore a particle in high viscosity environment will experience more resistance to motion resulting in a decrease in the speed at which the particle moves, and vice versa for the same particle in low viscosity solution. Last but not least, the temperature of the solution is another factor. Temperature is directly correlated to the entropy, so high temperature forces more movement between the particle and the solvent and result in faster diffusion speed than the particle at a lower temperature, and temperature can impact the viscosity of the solution.

The velocity of the Brownian motion is defined by the translational diffusion coefficient (D) and this piece of information is used in the Stokes-Einstein equation to provide hydrodynamic size⁴⁹. The hydrodynamic size means the diameter of the sphere that has the same average diffusion coefficient as the particle being measured⁵⁰. The equation for Stokes-Einstein is given in equation (1), by inspecting each term in equation, only the diffusion coefficient term is unknown, and the rest of the terms remains constant. As can be inferred by the equation,

having the diffusion coefficient term as denominator applies inverse relationship to the size. This relationship is intuitive since smaller particle size will move faster than the larger particle size.

$$d_H = \frac{kT}{3 \pi \eta D}, \text{ Equation (1)}$$

where d_H = hydrodynamic diameter, k = Boltzmann's constant, η = viscosity, and D = diffusion coefficient.

During the random motion of the particle, the laser source is constantly targeting a constant location of the sampling cuvette. Photons emitted by the laser collide with the mobile solute molecules and allow light scattering. The scattered light information will be collected over a very short time intervals, e.g., tens to hundreds of nanoseconds, by the detector unit. Over time, the intensity of scattered light fluctuates due to the random diffusion motion. These time depended light fluctuation are collected and correlated to allow calculation of the diffusion coefficient. The small particles undergo faster fluctuation scattered light and large particle size undergo slower fluctuation as shown schematically in Figure 18.

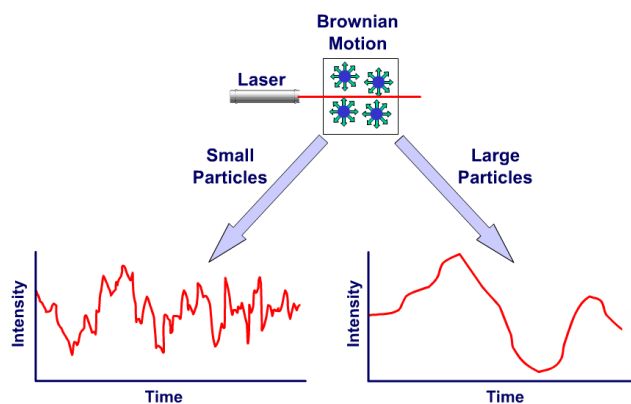


Figure 18. Time depended fluctuation of small and large particles.

The correlation can be comprehended as comparing the pictures of a particle in solution at time $t=0$, $t=t_1$, $t=t_2$, ... $t=t$, note that the scale of time in this function is in a microsecond. An image collected at $t=0$ as the base is then compared to subsequent images. The initial image will have a high correlation with the next image because after a very short time later (a few

nanoseconds) the particle has not yet moved much, resulting in an image that is very similar to the base. And, as time interval increases and the particles start to exhibit significant diffusional motion the correlation between images drastically decrease, as shown in the correlogram in Figure 19.

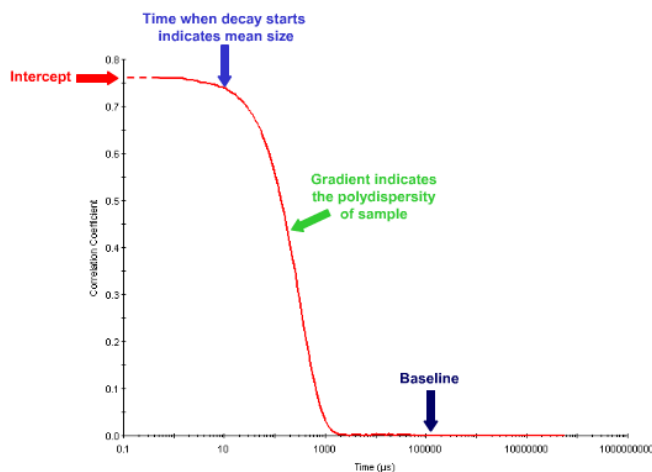


Figure 19. An example of a correlogram result.

The intercept value represents the signal to noise ratio, and the correlogram information can be transformed into information on the size distribution of the solution. It is very important to not only rely on size distribution information and observe the correlogram graph first because this graph represents the quality of the obtained size distribution values.

It is also important to note that the DLS is not a true measure of the MW of the polymer. Since for a given degree of polymerization or MW the polymer-solvent interaction will determine the hydrodynamic volume of the solvent swollen polymer, which is actually measured by the DLS.

All of the theory information was referenced from Chapter 11, DLS theory, from Malvern's Zetasizer DLS user manual⁴⁹

Common applications of DLS include the stability of polymer in surfactant solution⁵¹. Ricka, et al., 1989 studied the surfactant effect of sodium dodecyl sulfate on poly(*N*-

isopropylacrylamide) polymer using DLS. This work showed how an increase in surfactant concentration increased the stability of aggregation or prevent the collapse of polymers as a result higher hydrodynamic size.

Visual inspection of the solubility or stability of a polymer in a solvent not a reliable measurement. Therefore, quantitative tools such as the DLS are useful for measuring the solubility of the polymers, collides or suspensions. In this study, two commercial grade cellulose acetates investigated. These two samples were selected to be very similar in their acetyl DS and absolute MW, and MW distribution, but differed in the amount of insoluble gel particle. Many prior studies have shown the negative impact of these gel's on the overall processibility and product quality of cellulose esters⁵⁻⁷. This work was intended to evaluate the utility of DLS for measuring the impact of gels of the behavior of cellulose acetate solutions.

Experiment methods and materials

Materials

Two commercial grade cellulose acetates (CA) were supplied by Eastman Chemical Company. These samples were carefully selected to have the same DS and absolute MW, but differing amounts of gel particles. The samples were designated as CA-HQ and CA-LQ to indicate a higher and lower amount of gel, respectively, CA-LQ sample maintains about 5 time more amount of gel particle by weight compare to CA-HQ sample. All chemicals and materials were purchased from Fisher Scientific and used without further purifications.

Dynamic light scattering (DLS)

Zetasizer Nano ZS (Malvern Panalytical, Malvern UK) was used to perform DLS measurements. Each experiment was performed in triplicates, and the scan numbers for each replicate was between 12 and 16 scans. The attenuator and cell position settings also remained automatic settings for the best result.

Insoluble gel extraction

Cellulose acetate samples were prepared as 3 wt% solutions in acetone. Specifically, 900 mg of cellulose acetate and 29.1 g of acetone were mixed and left on an automatic shaker until complete dissolution was observed, typically 2 hours. The solution was transferred into 50 mL Falcon tubes and centrifuged at 4,400 rpm for 6 hr. The supernatant portion (1 g) was diluted to 0.5 wt% by mixing with additional acetone (5 g). The sediment ‘gels’ was washed with additional acetone to remove residual cellulose acetate. The washed gel was then used to prepare three different types of samples. First, the isolate gel was mixed with about 15 mL of acetone for DLS measurement. Second, the isolate gel was mixed with 19 g of 0.5 wt% CA for DLS measurement. Lastly, the gel was mixed with 60 g 0.5 wt% CA for DLS measurement. The detailed schematic of this procedure is shown on Figure 20.

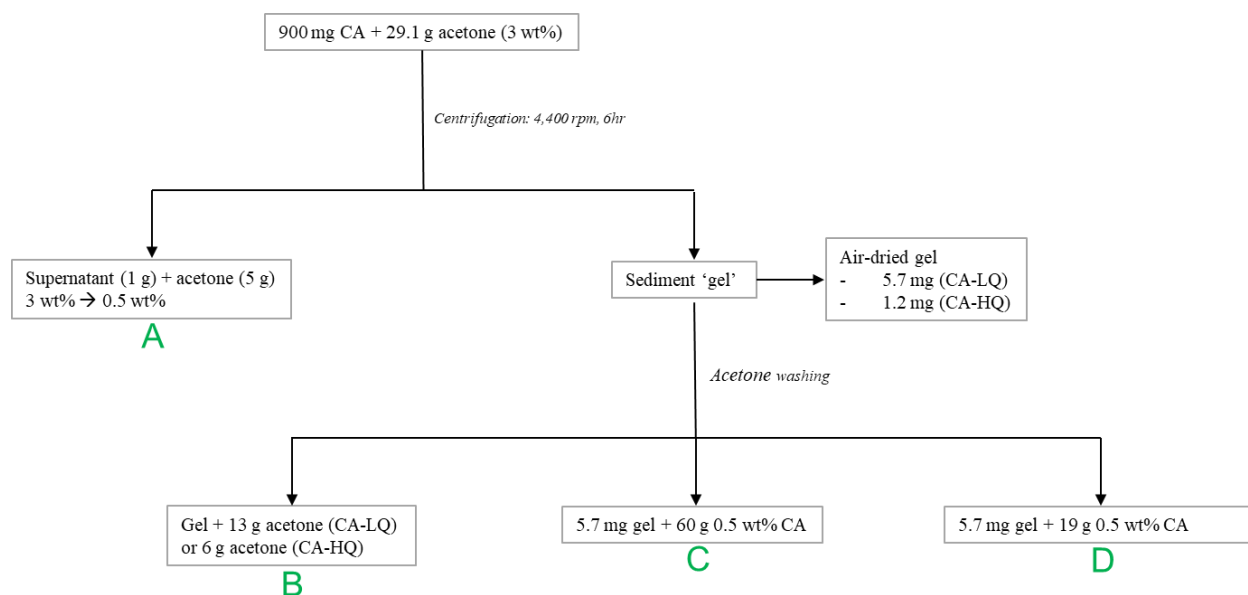


Figure 20. Schematic of cellulose acetate solution gel extraction and experimental method of each sample collecting point.

Result and discussion

The naming convention for the different samples is provided in

Table 9. The label of ‘high quality’ and ‘low quality’ is based on Eastman’s proprietary evaluation protocols. Then, the gel was air-dried overnight to evaporate the acetone and measured the weight of the gel. The CA-HQ yielded 1.2 mg of gel from 900 mg of CA-HQ, and CA-LQ yielded 5.7 mg of gel from 900 mg of CA-LQ.

Table 9. List of samples and descriptions for DLS experiment.

Name		Description	mg of gel
HQ.A	A	‘Gel free’ Supernatant 1g + acetone 5g	0
LQ.A		‘Gel free’ Supernatant 1g + acetone 5g	0
HQ.B	B	Gel isolated from CA-HQ + 6g acetone	1.2
LQ.B		Gel isolated from CA-LQ +13 g acetone	5.7
HQ.C	C	5.7 mg of CA-LQ gel + 60 g of 0.5 wt% CA-HQ in acetone	6.3
LQ.C		5.7 mg of CA-LQ gel + 60 g of 0.5 wt% CA-LQ in acetone	7.6
HQ.D	D	5.7 mg of CA-LQ gel + 19 g of 0.5 wt% CA-HQ in acetone	5.8
LQ-D		5.7 mg of CA-LQ gel + 19 g of 0.5 wt% CA-LQ in acetone	6.1

Baseline evaluation of the dynamic light scattering

Before conducting a detailed evaluation of the hydrodynamic size of the cellulose acetate samples with DLS, the instrument response was evaluated with a series of polystyrene standards. Two polystyrene (PS) standards with number average MWs of 13,000 g/mol and 290,000 g/mol, respectively, were used to evaluate the response of the Zetasizer. The response for the two samples is shown in Figure 21. Both samples were evaluated as 0.5 wt% solutions in tetrahydrofuran.

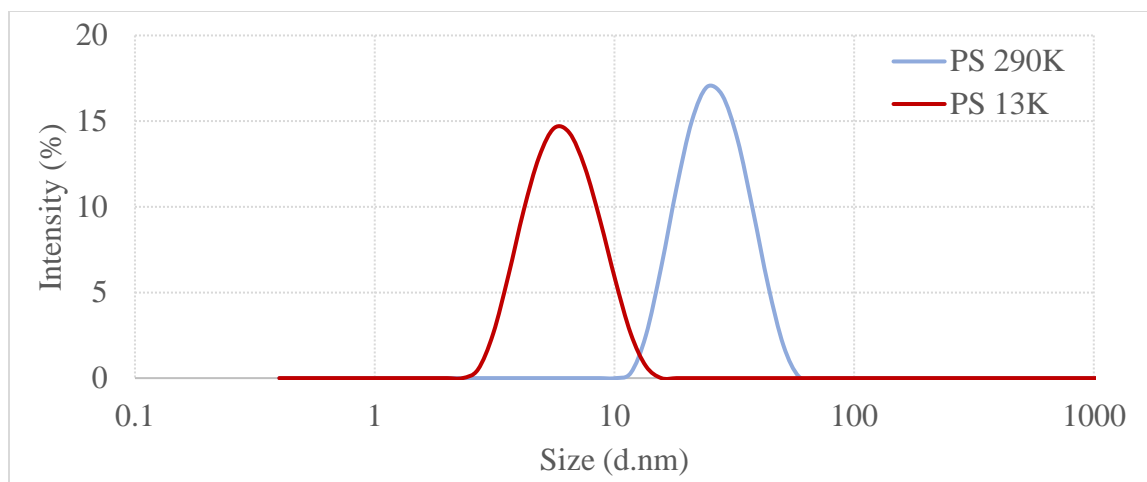


Figure 21. Size distribution by intensity graph for polystyrene materials

As expected the lower MW sample (PS-13K) resulted in a lower hydrodynamic diameter (6.4 nm) compared to the higher MW sample (PS-290) which has a hydrodynamic diameter of 27 nm. This difference in hydrodynamic size ensures the trustworthy and quality of the hydrodynamic size information produced by the instrument.

Next, the two PS samples were then mixed at a ratio of two parts of the low MW sample and one part of the high MW sample to create a third sample. These results are shown on Figure 22. As expected the DLS shows a bimodal response for both of the polystyrene standard materials, resulted sizes for two peaks are 5.6 nm and 32 nm.

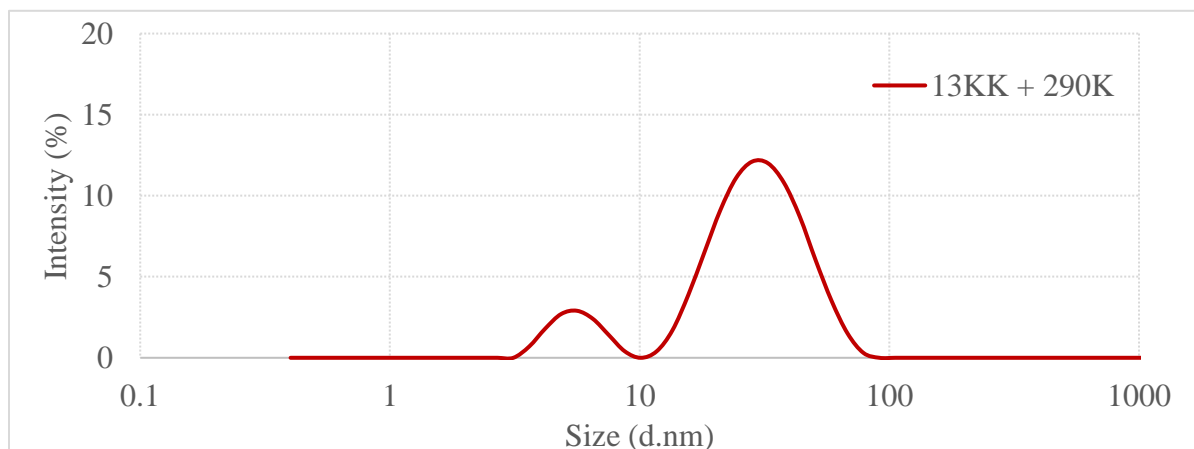


Figure 22. A mixture of PS-13K and PS-290K.

The DLS response for the PS mixtures suggests that the CA solutions with varying amounts of a second component with a larger hydrodynamic volume, e.g., gel particles, can be detected with the DLS.

DLS of CA-HQ and CA-LQ

CA samples of both HQ and LQ, before gel removal, were prepared as 0.5 wt% solutions in acetone. The result of DLS for both samples is shown in Figure 23. As expected there are subtle differences between the two samples. The calculated hydrodynamic diameter for HQ and LQ samples are 594 nm and 642 nm, respectively. This was expected due to the higher amount of gel present in the LQ sample. based on our prior work, and the literature, we expect these gel particles to have a larger hydrodynamic diameter themselves, and also increase the viscosity of the CA solutions due to aggregation effects.^{5, 47}

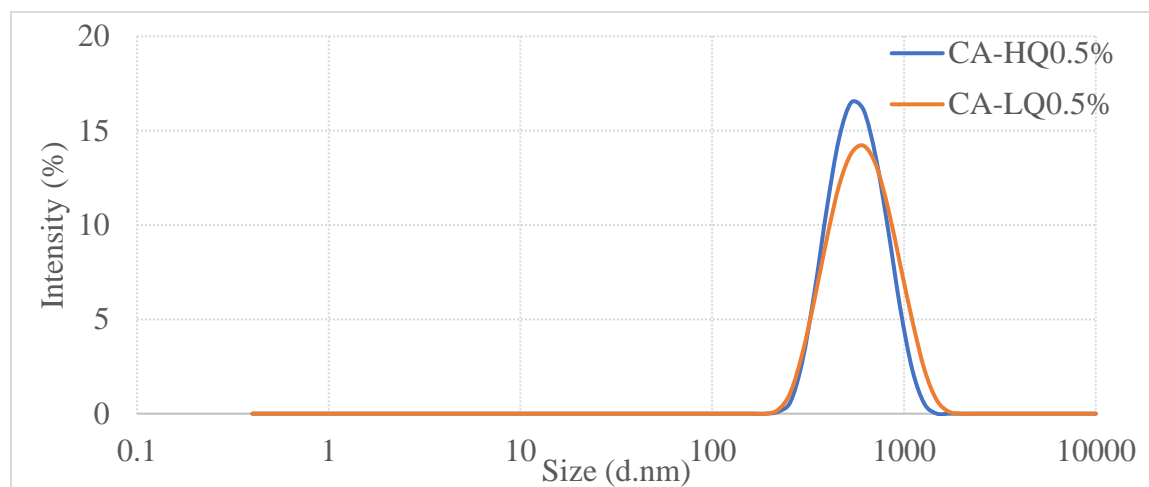


Figure 23. DLS measurement for CA-HQ and LQ before gel removal.

Another interesting result that was found from DLS is the linear relationship between concentrations of the sample and the calculated diameters. Table 10 shows the list of different wt% concentration ranging from 0.1 – 1.0%. One master batch of 1.0 wt% solution was made by

mixing 300 mg of CA-HQ or LQ and 29.7 g acetone. Then, 1 mL of aliquot was mixed with listed grams of acetone from the table to dilute to the desired level of wt %.

Table 10. Amount of acetone added to dilute 1.0% to 0.1 - 0.9% solutions. (All samples were diluted from 1 wt % solution, 300mg CA + 29.7 g acetone).

<i>Sample</i>	<i>g Acetone</i>	<i>D_H (d.nm)</i>	<i>Diffusion coefficient</i>
HQ-0.1%	7.13	403	3.89
HQ-0.3%	1.85	513	3.06
HQ-0.5%	0.79	594	2.67
HQ-0.7%	0.34	765	2.09
HQ-1.0%	0	1021	1.53
LQ-0.1%	7.13	422	3.99
LQ-0.3%	1.85	525	3.08
LQ-0.5%	0.79	642	2.61
LQ-0.7%	0.34	800	2.03
LQ-1.0%	0	1064	1.57

The hydrodynamic size responses for each concentration have the same trend that the increase in sample concentration led to an increase in sizes. It is possible that the change in solution viscosity was the driver of this change. The viscosity of the solution can change noticeably when a high molecular weight polymer like cellulose acetate is dissolved. As more cellulose acetate is dissolved in acetone the solution viscosity increases, which will slow down the diffusion speed, with a resulting impact on the diffusion coefficient (Table 10). Recalling the equation (1) the diffusion coefficient term is in the denominator; therefore, it makes sense that an increase in the diffusion coefficient will decrease the hydrodynamic size. Also, it's important to note that difference between HQ and LQ at each concentration is consistent and all LQ samples have higher size values.

DLS comparison for gel particles and gel removed

To understand the impact of the presence of gel in cellulose acetate solutions, CA samples have been prepared targeting different concentration (ratio) of gel, Table 11. HQ.A and LQ.A samples both were prepared by using the supernatant portion after centrifuged, theoretically, there should not be any gel left so the gel ratio of 0 was given. HQ.B and LQ.B samples represent the centrifuged gel from CA-HQ (1.2 mg) and CA-LQ (5.7 mg) dispersed in acetone. Remaining two samples have been prepared by adding 5.7 mg of CA-LQ gel to each sample and the ratio values are different between HQ and LQ because the prepared CA for two sets haven't been centrifuged and there was some inherent amount of gel present.

Table 11. Gel ratio and hydrodynamic size for each sample.

Name	Gel ratio (mg gel / mg CA)	d_H (d.nm)
HQ.A	0.00	608
LQ.A	0.00	576
HQ.B	1.00	680
LQ.B	1.00	679
HQ.C	0.02	823
LQ.C	0.025	755
HQ.D	0.058	883
LQ.D	0.063	917

All samples from A, C, and D were prepared at 0.5 wt% solution, previous observation revealed the linear relationship between size and concentration, therefore all samples were prepared at the same mass concentration for a fair comparison. First, looking at the size results for HQ.A and LQ.A, gel free, it seems that the diameter for LQ.A have changed significantly but the size for HQ.A look to be unchanged. LQ-0.5% before gel removal had 640 nm and after the gel removal, the size dropped to 575 nm. The observed change agrees with the hypothesis from the previous chapter that xylan from the gel particle is capable of forming aggregation either among themselves or unreacted cellulose⁵. Chen, et al., 2013, proved a microcrystalline structure of cellulose present within the gel for the sample with a heavy amount of xylan composed gel.

Thereby, removing the gel particles means removing all aggregates that can appear to have a higher hydrodynamic diameter. One possible reason for unchanged diameter for a high quality sample is that from the beginning, there was a very small amount of gel present at an early stage, so the effect of gel aggregate is relatively less severe than LQ sample. HQ has almost 5 times less amount of gel present.

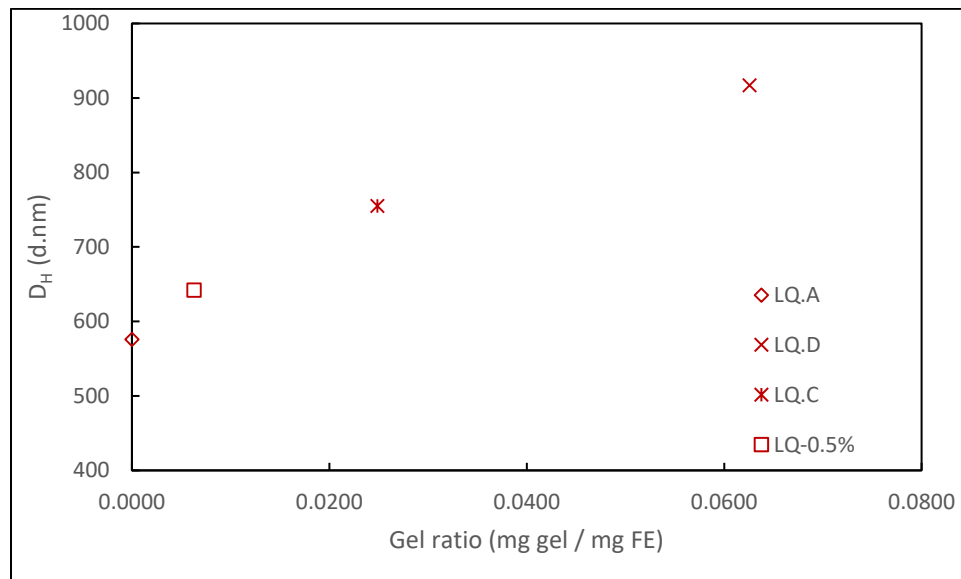


Figure 24. CA-LQ with different amount of gels.

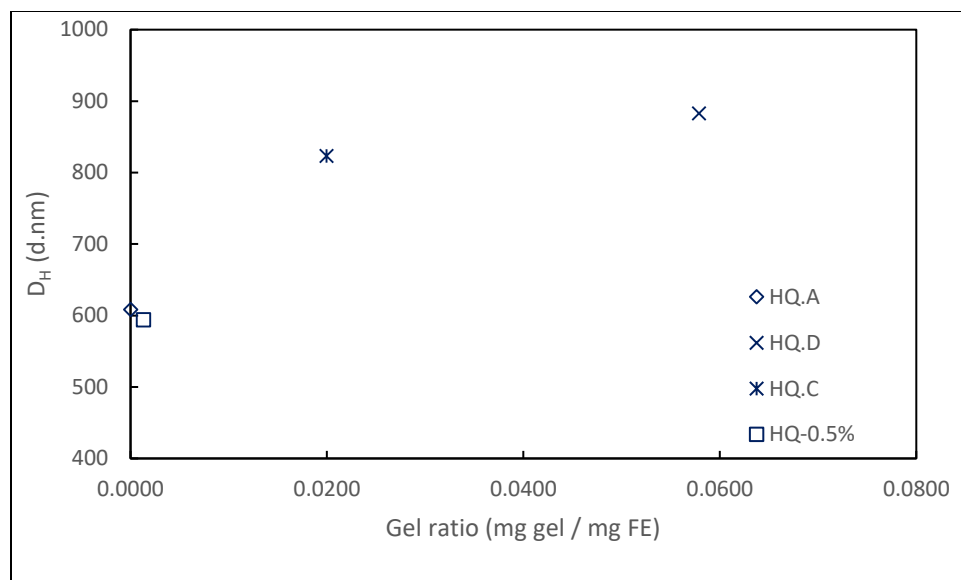


Figure 25. CA-HQ with different amount of gels.

Figure 24 and Figure 25 show the effect of different gel ratio on the size. It is clear that the amount of gel ratio increases by external addition also increased the hydrodynamic size for both samples. This size increase can be interpreted as promoting larger aggregate formation due to the larger amount of gel present. This finding supports the actual processability issue cellulose acetate producing industries are experiencing. Prior work by Bradway⁷ reported that gel particle can cause pore clogging issue during the filtration process. A larger amount of hemicellulose leads to more severe filterability issue. The observation from size increasing trend observed from above figures correlates with issues described from the previous report. A larger amount of hemicellulose causes DLS to detect larger size particle, and such a size can easily clog the filtering pore compared to the sample with less hemicellulose and smaller size.

Protocol for estimating the amount of gel particle present

After such a discovery, it was important to seek out for a possibility of measuring how much gel is present within the sample by DLS measurement. The easiest way to compare the result would be by comparing the size of different qualities of cellulose acetates. However, due to the sensitivity of size changing linearly with the concentration. A sort of calibration curve was made by plotting sizes of samples at the small difference in concentrations.

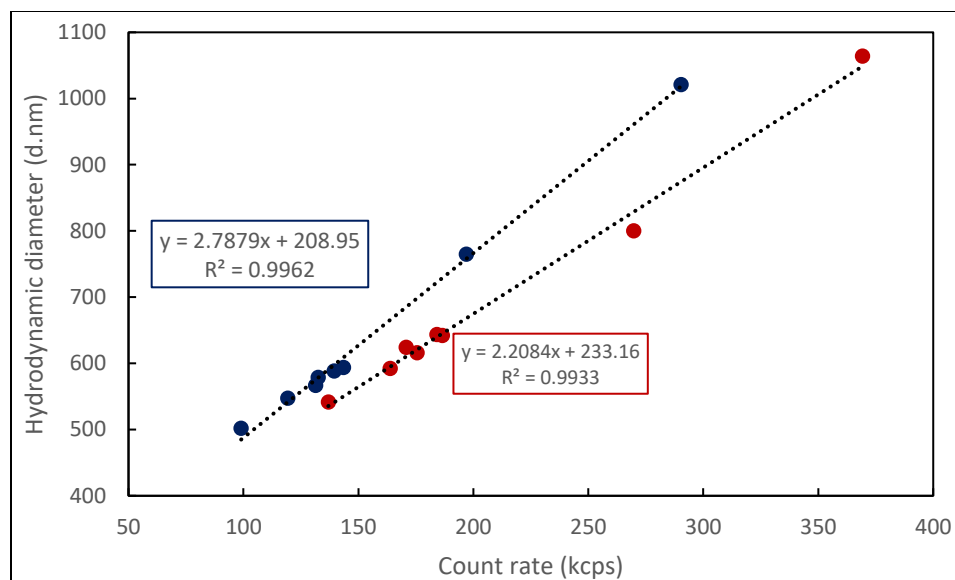


Figure 26. Calibration curves for CA-LQ (red) and CA-HQ (blue) to determine the amount of gel.

Above Figure 26 shows the linear regression graph for both CA-LQ and CA-HQ and 7 different concentrations were used (0.36, 0.42, 0.44, 0.45, 0.48, 0.5, 0.7, and 1.0%). All dilution solution was derived from a 1.0 wt% solution and diluted down to the desired level of concentration by adding acetone. First, it's interesting how a small change in concentration from 0.5 to 0.42% can accordingly result in responsive linearly decreasing size. Note the different x-axis value, a count rate. The count rate is a measure of how much laser photon is detected by the detector in kilo counts per second. Therefore, the underlying hypothesis is that larger particle size has a larger surface area that can interact with emitted photons and reflect more photons to the detector. And, surprisingly the relationship between count rate and hydrodynamic diameter is linearly correlated with R^2 value of 0.99 for both plots. The developed potential protocol to determine the amount of gel particle present is by comparing the intercept of both plots. Continuously the LQ sample had a slightly higher diameter and the similar difference is observed with the intercept value. Therefore, this is the proposing protocol that using concentration dilution plot of cellulose acetate samples and comparing the intercept values by means of determining the amount of gel particle present within the cellulose acetates with an unknown amount of gel particles. The result can be validated by centrifuging 3 wt% cellulose acetate solution.

Conclusion

Two different quality cellulose acetate samples were obtained to be examined through DLS. Both samples were dissolved in acetone at 0.5 wt% to measure the hydrodynamic sizes. It was discovered that the concentration gradient of CA in acetone led to a linear change in the sizes. Therefore, 0.5 wt% was fixed for all other comparisons in order to compare samples fairly. Comparing gel free CA solution and gel heavy CA solution revealed that as the amount of gel increased also increased the resulting sizes. This increase in size allowed us to better understand the impact of gel during the filtration process of commercial cellulose acetate industry. At last, applying the concentration and size linear relationship, a potential protocol was developed to estimate the amount of gel in cellulose acetate by comparing the intercept values. The actual feasibility of this protocol needs to be examined with more than two samples.

REFERECE

1. Kuo, C. M. K., TN), Bogan, Richard T. (Kingsport, TN) Process for the manufacture of cellulose acetate. 1997.
2. Malm, C. J.; Tanghe, L. J.; Laird, B. C., Preparation of Cellulose Acetate - Action of Sulfuric Acid. *Industrial & Engineering Chemistry* **1946**, 38 (1), 77-82.
3. Araki, T., Studies on Cellulose Acetate:Part III: Combination of Sulfuric Acid During the Acetylation of Cellulose and the Mechanism of Acetylation. *Textile Research Journal* **1952**, 22 (10), 630-636.
4. McCormick, C. L.; Callais, P. A., Derivatization of cellulose in lithium chloride and N-N-dimethylacetamide solutions. *Polymer* **1987**, 28 (13), 2317-2323.
5. Chen, X. L.; Xu, S. W.; Peng, W. J.; Zhang, J.; Jiang, Y., Isolation and characterization of acetone-insoluble substances in cellulose acetate prepared by an acetic acid acetylation process. *Cellulose chemistry and technology* **2013**, 48, 477-483.
6. Fleury, E.; Dubois, J.; Léonard, C.; Joseleau, J. P.; Chanzy, H., Microgels and ionic associations in solutions of cellulose diacetate. *Cellulose* **1994**, 1 (2), 131-144.
7. Bradway, K. E. An Investigation of Haze in Cellulose Acetates Made from Wood Pulps. Lawrence College, Appleton, Wisconsin, 1953.
8. Wilson, J. D.; Tabke, R. S., Influences of hemicelluloses on acetate processing in high catalyst systems. In *TAPPI*, Atlanta, GA, 1973; pp 55-67.
9. Gardner, P.; Chang, M., Acetylation of Native and Modified Hemicelluloses. *Tappi* **1974**, 57 (8), 71-75.
10. Kim, C. H.; Lee, J.; Treasure, T.; Skotty, J.; Floyd, T.; Kelley, S. S.; Park, S., Alkaline extraction and characterization of residual hemicellulose in dissolving pulp. *Cellulose* **2018**.
11. Masao Horio, R. I., Crystallographic Study of Xylan from Wood. *Journal of Polymer Science Part A: General Papers* **1964**, 2 (2), 627-644.
12. Chen, C.; Duan, C.; Li, J.; Liu, Y.; Ma, X.; Zheng, L.; Stavik, J.; Ni, Y., *Cellulose (Dissolving Pulp) Manufacturing Processes and Properties: A Mini-Review*. 2016; Vol. 11.
13. Kumar, H.; Christopher, L. P., Recent trends and developments in dissolving pulp production and application. *Cellulose* **2017**, 24 (6), 2347-2365.

14. Rosenau, T.; Potthast, A.; Sixta, H.; Kosma, P., The chemistry of side reactions and byproduct formation in the system NMMO/cellulose (Lyocell process). *Progress in Polymer Science* **2001**, *26* (9), 1763-1837.
15. Adorjan, I.; Potthast, A.; Rosenau, T.; Sixta, H.; Kosma, P., Discoloration of cellulose solutions in N-methylmorpholine-N-oxide (Lyocell). Part 1: Studies on model compounds and pulps. *Cellulose* **2005**, *12* (1), 51-57.
16. Öztürk, H. B.; Potthast, A.; Rosenau, T.; Abu-Rous, M.; MacNaughtan, B.; Schuster, K. C.; Mitchell, J. R.; Bechtold, T., Changes in the intra- and inter-fibrillar structure of lyocell (TENCEL®) fibers caused by NaOH treatment. *Cellulose* **2008**, *16* (1), 37.
17. Whistler, R. L., Xylan. *Advances in Carbohydrate Chemistry* **1950**, *5*, 286-287.
18. Arnoul-Jarriault, B.; Lachenal, D.; Chirat, C.; Heux, L., Upgrading softwood bleached kraft pulp to dissolving pulp by cold caustic treatment and acid-hot caustic treatment. *Industrial Crops and Products* **2015**, *65*, 565-571.
19. Duan, C.; Li, J. G.; Ma, X. J.; Chen, C. X.; Liu, Y. S.; Stavik, J.; Ni, Y. H., Comparison of acid sulfite (AS)- and prehydrolysis kraft (PHK)-based dissolving pulps. *Cellulose* **2015**, *22* (6), 4017-4026.
20. Sixta, H., *Handbook of Pulp*. Wiley-vch: New York, 2006.
21. Bajpai, P., Chapter 12 - Pulping Fundamentals. In *Biermann's Handbook of Pulp and Paper (Third Edition)*, Bajpai, P., Ed. Elsevier: 2018; pp 295-351.
22. Stepan, A. M.; King, A. W. T.; Kakko, T.; Toriz, G.; Kilpelainen, I.; Gatenholm, P., Fast and highly efficient acetylation of xylans in ionic liquid systems. *Cellulose* **2013**, *20* (6), 2813-2824.
23. A. Sluiter; B. Hames; R. Ruiz; C. Scarlata; J. Sluiter; D. Templeton; Crocker, D. *Determination of Structural Carbohydrates and Lignin in Biomass*; National Renewable Energy Laboratory: 8/3/2012, 2012.
24. Ostonen, A.; Bervas, J.; Uusi-Kyyny, P.; Alopaeus, V.; Zaitsau, D. H.; Emel'yanenko, V. N.; Schick, C.; King, A. W. T.; Helminen, J.; Kilpelainen, I.; Khachatryan, A. A.; Varfolomeev, M. A.; Verevkin, S. P., Experimental and Theoretical Thermodynamic Study of Distillable Ionic Liquid 1,5-Diazabicyclo[4.3.0]non-5-enium Acetate. *Industrial & Engineering Chemistry Research* **2016**, *55* (39), 10445-10454.

25. Esbensen, K. H., *An introduction to multivariate data analysis and experimental design*. 5 ed.; Esbjerg.
26. Geladi, P.; Kowalski, B. R., Partial least-squares regression: a tutorial. *Analytica Chimica Acta* **1986**, *185*, 1-17.
27. Kakko, T.; King, A. W. T.; Kilpeläinen, I., Homogenous esterification of cellulose pulp in [DBNH][OAc]. *Cellulose* **2017**, *24* (12), 5341-5354.
28. Grondahl, M.; Teleman, A.; Gatenholm, P., Effect of acetylation on the material properties of glucuronoxylan from aspen wood. *Carbohydrate Polymers* **2003**, *52* (4), 359-366.
29. Goodlett, V. W.; Dougherty, J. T.; Patton, H. W., Characterization of cellulose acetates by nuclear magnetic resonance. *Journal of Polymer Science Part A-1: Polymer Chemistry* **1971**, *9* (1), 155-161.
30. Fundador, N. G. V.; Enomoto-Rogers, Y.; Takemura, A.; Iwata, T., Acetylation and characterization of xylan from hardwood kraft pulp. *Carbohydrate Polymers* **2012**, *87* (1), 170-176.
31. Fei, P.; Liao, L.; Cheng, B.; Song, J., Quantitative analysis of cellulose acetate with a high degree of substitution by FTIR and its application. *Analytical Methods* **2017**, *9* (43), 6194-6201.
32. Kačuráková, M.; Capek, P.; Sasinková, V.; Wellner, N.; Ebringerová, A., FT-IR study of plant cell wall model compounds: pectic polysaccharides and hemicelluloses. *Carbohydrate Polymers* **2000**, *43* (2), 195-203.
33. Timell, T. E., Recent progress in the chemistry of wood hemicelluloses. *Wood Science and Technology* **1967**, *1* (1), 45-70.
34. Holtzapple, M. T., HEMICELLULOSES. In *Encyclopedia of Food Sciences and Nutrition (Second Edition)*, Caballero, B., Ed. Academic Press: Oxford, 2003; pp 3060-3071.
35. Farhat, W.; Venditti, R. A.; Hubbe, M.; Taha, M.; Becquart, F.; Ayoub, A., A Review of Water-Resistant Hemicellulose-Based Materials: Processing and Applications. *ChemSusChem* **2017**, *10* (2), 305-323.
36. Bailey, R. W.; Pickmere, S. E., Alkali solubility of hemicelluloses in relation to delignification. *Phytochemistry* **1975**, *14* (2), 501-504.

37. Xu, F.; Sun, J. X.; Geng, Z. C.; Liu, C. F.; Ren, J. L.; Sun, R. C.; Fowler, P.; Baird, M. S., Comparative study of water-soluble and alkali-soluble hemicelluloses from perennial ryegrass leaves (*Lolium perene*). *Carbohydrate Polymers* **2007**, *67* (1), 56-65.
38. Aracri, E.; Díaz Blanco, C.; Tzanov, T., An enzymatic approach to develop a lignin-based adhesive for wool floor coverings. *Green Chemistry* **2014**, *16* (5), 2597-2603.
39. Fang, J. M.; Sun, R. C.; Tomkinson, J.; Fowler, P., Acetylation of wheat straw hemicellulose B in a new non-aqueous swelling system. *Carbohydrate Polymers* **2000**, *41* (4), 379-387.
40. Pettolino, F. A.; Walsh, C.; Fincher, G. B.; Bacic, A., Determining the polysaccharide composition of plant cell walls. *Nature Protocols* **2012**, *7*, 1590.
41. Lee, C.; Dazen, K.; Kafle, K.; Moore, A.; Johnson, D. K.; Park, S.; Kim, S. H., Correlations of Apparent Cellulose Crystallinity Determined by XRD, NMR, IR, Raman, and SFG Methods. In *Cellulose Chemistry and Properties: Fibers, Nanocelluloses and Advanced Materials*, Rojas, O. J., Ed. Springer International Publishing: Cham, 2016; pp 115-131.
42. Johar, N.; Ahmad, I.; Dufresne, A., Extraction, preparation and characterization of cellulose fibres and nanocrystals from rice husk. *Industrial Crops and Products* **2012**, *37* (1), 93-99.
43. Filho, G. R.; da Cruz, S. F.; Pasquini, D.; Cerqueira, D. A.; Prado, V. d. S.; de Assunção, R. M. N., Water flux through cellulose triacetate films produced from heterogeneous acetylation of sugar cane bagasse. *Journal of Membrane Science* **2000**, *177* (1), 225-231.
44. Miller, R. L.; Boyer, R. F.; Heijboer, J., X-ray scattering from amorphous acrylate and methacrylate polymers: Evidence of local order. *Journal of Polymer Science: Polymer Physics Edition* **1984**, *22* (12), 2021-2041.
45. Barud, H. S.; de Araújo Júnior, A. M.; Santos, D. B.; de Assunção, R. M. N.; Meireles, C. S.; Cerqueira, D. A.; Rodrigues Filho, G.; Ribeiro, C. A.; Messaddeq, Y.; Ribeiro, S. J. L., Thermal behavior of cellulose acetate produced from homogeneous acetylation of bacterial cellulose. *Thermochimica Acta* **2008**, *471* (1), 61-69.
46. Hindeleh, A. M.; Johnson, D. J., Peak resolution and X-ray crystallinity determination in heat-treated cellulose triacetate. *Polymer* **1972**, *13* (1), 27-32.

47. Andrewartha, K. A.; Phillips, D. R.; Stone, B. A., Solution properties of wheat-flour arabinoxylans and enzymically modified arabinoxylans. *Carbohydrate Research* **1979**, *77* (1), 191-204.
48. Linder, Å.; Bergman, R.; Bodin, A.; Gatenholm, P., Mechanism of Assembly of Xylan onto Cellulose Surfaces. *Langmuir* **2003**, *19* (12), 5072-5077.
49. Size Theory. In *Zetasizer Nano User Manual*, Malvern Instrument: Worcestershire, United Kingdom, 2013; Vol. 4, pp 215-222.
50. Peccora, R., *Dynamic Light Scattering: Application of photon correlation spectroscopy*. Plenum Press: New York, NY, 1985.
51. Rika, J.; Meewes, M.; Nyffenegger, R.; Binkert, T., Intermolecular and intramolecular solubilization: Collapse and expansion of a polymer chain in surfactant solutions. *Physical Review Letters* **1990**, *65* (5), 657-660.